Analysis of the arbitrary Mindlin plate by spline finite strip method

by

Xie Chen

A thesis
Submitted to the School of Graduate Studies and Research
University of Ottawa
in partial fulfilment of the
requirements for the degree of
Master of Applied Science
in
Civil Engineering
Under the auspices of the Ottawa-Carleton
Institute for Civil Engineering

ISBN 0-315-83812-4

UNIVERSITÉ D'OTTAWA
UNIVERSITY OF OTTAWA

Acknowledgement

The author wishes to express his sincere gratitude to Professor S.F.Ng for his supervision, constructive criticism and generous support throughout the course of this work. Acknowledgement is also extended to my colleagues W.C.Li and J.Q.Zhou for their assistance and fruitful discussion.

The author would like to give special thanks to his wife Xiao-Qi Huang for her patience, fortitude and support during my course of graduate studies.

Contents

Chapter 1

Introduction

1.1. General

In recent years, due to site restrictions and/or the impact of the environment, more and more short to medium span bridges have an arbitrary shape. These bridges are very often curved along two sides while the abutment or piers are skewed. In some cases, they are continuous for several spans and can even be 'S'-shaped in plan. These complications often lead to difficulties, and recourse usually has to be made to numerical techniques, such as finite element and grillage analysis. Also, with

modern design of concrete bridge decks, the thickness of the slab may be such that the influence of transverse shear on the deformations and stresses is significant. It is well known that, if the classical thin plate theory is applied to analyze moderately thick bridge decks, the effect of transverse shear deformation cannot be taken into account and the simple Kirchhoff theory may yield results that are unacceptable for engineering design. The motivation here is to find a sufficiently accurate numerical method that would enable an efficient analysis of arbitrary shaped and moderately thick plates or bridge decks.

1.2. Object and scope

The main objective of the thesis is to extend the spline finite strip method to analyze moderately thick plates or bridge decks. The efficiency and accuracy of this new numerical technique is demonstrated by numerical examples for both thin and thick plates of arbitrary planforms with or without intermediate supports and subjected to both uniform and concentrated loads.

1.3. Outline of the thesis

Since the main objective of this thesis is to use the spline finite strip method

to analyze arbitrary shaped Mindlin plates, the refined elastic plate theories are reviewed in Chapter 2. As a comparison, in the same Chapter, the classical elastic plate method is also reviewed. Chapter 3 is a brief literature review of the finite strip method and the spline finite strip method. Chapter 4 is devoted to the formulation of all equations for the analysis of arbitrary Mindlin plates by the spline finite strip method. Chapter 5 outlines the Gauss numerical integration and penalty function methods. Both of these techniques are widely used in numerical analysis in recent years, and are the vital tools in the analysis of arbitrary Mindlin plates. Chapter 6 shows numerical examples which are used to demonstrate the accuracy and, in particular, the simplicity and efficiency of the spline finite strip method. The last Chapter is devoted to discussions and conclusions for the present study.

For all cases considered in this study, whenever possible, comparisons are made with other investigators. All computations involved in this thesis were programmed in Fortran and the program is included in Appendix A. Since one of the major advantages of the present method over the conventional finite element method lies in its simplicity in input data preparation, comparison of data input for a fan shaped bridge example as shown in Fig.6.1 is included in Appendix B.

Chapter 2

Classical and refined theories of elastic plates

2.1. Classical elastic plate theory

In the classical thin plate theory, based on the Kirchhoff assumption, points on the midsurface z=0 move in the z direction only as the plate deforms in bending. A line that is straight and normal to the midsurface before loading is assumed to remain straight and normal to the midsurface after loading (see line OP in Fig.2.1). Thus, transverse shear deformation is assumed to be zero. A point not on the

midsurface has displacement components u and v in the x and y directions, respectively. From Fig.2.1, for small angles of rotation,

$$u=-z\frac{\partial w}{\partial x} \quad ; \quad v=-z\frac{\partial w}{\partial y} \quad \text{hence} \quad \begin{aligned} \epsilon_x &= \frac{\partial u}{\partial x} &&= -z\frac{\partial w^2}{\partial^2 x} \\ \epsilon_y &= \frac{\partial v}{\partial y} &&= -z\frac{\partial^2 w}{\partial y^2} \\ \gamma_{xy} &= \frac{\partial u}{\partial y} + \frac{\partial v}{\partial x} &&= -2z\frac{\partial^2 w}{\partial x \partial y} \end{aligned} \qquad (2.1)$$

The governing differential equation for the isotropic homogeneous thin plate undergoing small deflection is:

$$\frac{\partial^4 w}{\partial x^4} + 2\frac{\partial^4 w}{\partial x^2 \partial y^2} + \frac{\partial^4 w}{\partial y^4} = q/D \qquad (2.2)$$

where w is the transverse deflection of the plate; q is the applied transverse load; and $D=Eh^3/12(1-\nu^2)$ is the flexural rigidity of the plate, where E and ν are the modulus of elasticity and Poisson's ratio, respectively; and h is the plate thickness. In Equation(2.2) the influence of transverse shear strains is neglected.

It is well known that for many technical applications, the classical theory of plates yields sufficiently accurate results. However, there exist a fairly large class

of engineering problems where results given by the simple Kirchhoff's thin plate equation are unacceptable. This fact is obviously due to the initial simplifying assumptions adopted in the classical theory for plate bending. Analogous to the Bernoulli-Navier's beam which loses its truthfulness with the increasing ratio of the height of the cross section to the span of the beam considered, the accuracy of the classical thin plate theory also decreases with the growing thickness of the plate.

The imperfections of the classical theory mentioned above have caused various authors to develop new, more accurate theories for elastic plates, the best known of which were established by E.Reisser [5,6], H.Hencky [7], A.Kromm [8,9] and R.D.Mindlin [3].

2.2. Mindlin plate theory

Mindlin Plate Theory was first published by R.D.Mindlin in 1951. Mindlin plate elements account for both bending deformation and transverse shear deformations. In the Mindlin plate theory, a straight line originally normal to the mid-plane of the plate remains straight but may not be normal to this plane after deformation. In reality such a line is generally curved but the assumed straight, non-normal line can closely approximate this curved line in an average sense at all points. A shear correction factor is introduced to take account of the fact that the shear

strain distribution through the plate thickness is not uniform; for isotropic materials this shear correction factor is usually taken to be $\pi^2/12$ in the Mindlin theory. The Mindlin assumptions for plate bending can be stated simply as follows:

1. The lateral deflections of the plate, w are small.
2. Normals to mid-plane of the plate before deformation remain straight but not necessarily normal to the mid-plane after deformation.
3. The stress normal to the mid-plane, σ_z is negligible.

Thus, transverse shear deformation is allowed. The motion of a point not on the mid-plane is not governed by slopes $w_{,x}$ and $w_{,y}$ as in the Kirchhoff theory. Rather, its motion depends on rotations θ_x and θ_y of lines that were normal to the midplane of the underformed plate (Fig.2.2). Thus, with θ_x and θ_y being small angles of rotation,

$$\begin{aligned} u &= -z\theta_x \\ v &= -z\theta_y \\ w &= w(x,y) \end{aligned} \tag{2.3}$$

so the strain-displacement equation can be obtained as:

$$\begin{aligned} \varepsilon_x &= \frac{\partial u}{\partial x} = -z\frac{\partial \theta_x}{\partial x} & \gamma_{xy} &= \frac{\partial u}{\partial y} + \frac{\partial v}{\partial x} = -z\left(\frac{\partial \theta_x}{\partial y} + \frac{\partial \theta_y}{\partial x}\right) \\ \varepsilon_y &= \frac{\partial v}{\partial y} = -z\frac{\partial \theta_y}{\partial y} & \gamma_{yz} &= \frac{\partial w}{\partial y} + \frac{\partial v}{\partial z} = \frac{\partial w}{\partial y} - \theta_y \\ & & \gamma_{zx} &= \frac{\partial w}{\partial x} + \frac{\partial u}{\partial z} = \frac{\partial w}{\partial x} - \theta_x \end{aligned} \tag{2.4}$$

and also the stress can be expressed as:

$$\begin{aligned} \sigma_x &= a_1\varepsilon_x + a_2\varepsilon_y \\ \sigma_y &= b_1\varepsilon_x + b_2\varepsilon_y \\ \tau_{xy} &= c_1\gamma_{xy} \quad \tau_{yz} = c_2\gamma_{yz} \quad \tau_{xz} = c_3\gamma_{xz} \end{aligned} \tag{2.5}$$

where, for an isotropic homogeneous plate,

$$a_1 = b_2 = \frac{E}{1-\nu^2}, \qquad and \qquad a_2 = b_1 = \frac{\nu E}{1-\nu^2} \tag{2.6}$$
$$c_1 = G \qquad c_2 = c_3 = \kappa G$$

in which, E, ν are defined following equation (2.2), G is the shear modulus and κ is the shear correction factor.

Equations (2.4) are the strain-displacement relations of the Mindlin plate theory. The theory accounts for the effect of transverse shear deformation and is therefore especially applicable to the analysis of moderately thick plates.

2.3. Finite strip Method

The finite Strip method is a semi-analytical method. The method was first

published by Y.K.Cheung [37] for the analysis of simply supported bridge deck structures in 1968. For analyzing regular bridge decks, the finite strip method has proven to be the most efficient numerical method. The method utilizes a series of orthogonal functions in the longitudinal direction combined with the conventional finite element polynomial shape functions in the transverse direction to simulate all the displacement components of the structure. Basically, the method is a hybrid procedure which retains advantages of both the orthotropic plate method and the finite element concept.

For example, for a simply supported rectangular plate, in one strip (Fig.2.3), the deflection is expressed as:

$$w(x,y)=\sum_{m=1}^{r} f_m(x)\sin\frac{m\pi y}{a}=\sum_{m=1}^{r}(A+Bx+CX^2+DX^3+...)\sin\frac{m\pi y}{a} \qquad (2.7)$$

where A,B,C, ..., are undetermined coefficients, m represents the mth harmonic, and r stands for the specified number of harmonics to be used for the solution. Thus, the number of dimensions of the analysis is reduced by at least one. Consequently, the computer time, storage and input data are reduced significantly.

2.4. Spline finite strip method

The semi-analytical finite strip method is very efficient for the analysis of prismatic structures under distributed loading, especially for structures with both ends simply supported. Nevertheless, the use of this method can sometimes lead to difficulties. For instance, because the beam functions are continuously differentiable, it is difficult to use such functions to simulate the abrupt changes of bending moment at internal supports or at loaded cross-sections of point forces. In addition, the beam functions must satisfy the end conditions of a strip a priori; hence, these functions cannot deal with discrete supports at strip ends.

In order to overcome these difficulties, the mathematical tool called 'B_3-spline' was used as the longitudinal displacement functions to form the spline finite strips for the analysis of rectangular plates by Y.K.Cheung et al [10] in 1982. By using such spline functions to replace the function series, the above problems can be overcome, because a suitable spline function with the required continuity (discontinuity) conditions can always be found. Furthermore, similar to the finite element method, a spline finite strip can take up any prescribed external and internal boundary conditions, for example, by a penalty function approach. Thus, the spline strip method is more flexible than the semi-analytical finite strip method in imposing boundary conditions.

The spline, which was originally the name of a small flexible wooden strip employed by draughtsman as a tool for drawing a continuous smooth curve segment by segment, became a mathematical tool only after the work of Schoenberg [11]. It was further developed by Ahlberg et al [12], Greville [13], Schultz [14], Birkhoff & de Boor [15] and others, but unfortunately it has attracted little attention from engineering analysts until it was highlighted by Prenter [16].

A variety of spline functions are available. In most references, the B_3-spline is chosen to represent the longitudinal variation of displacements. This function is a piecewise cubic polynomial with continuity up to the second derivative. For one dimensional interpolation, in each section, the value of f(y) is related to four splines which are centred at the two ends of this section and the two additional knots next to the ends. Therefore, two additional knots are needed to interpolate f(y) in the first and last sections and is given (Fig.2.4) by:

$$f(y) = \sum_{i=-1}^{m+1} \alpha_i \varphi_i \qquad (2.8)$$

in which each local B_3-spline φ_i has non-zero values over four consecutive sections. In order to use spline functions to interpolate an arbitrary function f(y) on the interval $a \le y \le b$, the interval may be divided into a number of sections by equally

spaced knots y_m ($0 \le m \le r$, $y_0=a$, $y_r=b$, $y_m = y_0 + m(b-a)/r$). The equally spaced spline function f(y) with $y=y_m$ as the centre is defined by:

$$\phi_m(y) = \frac{1}{6h^3}\begin{cases} (y-y_{m-2})^3 & y_{m-2} \le y \le y_{m-1} \\ h^3+3h^2(y-y_{m-1})+3h(y-y_{m-1})^2-3(y-y_{m-1})^3 & y_{m-1} \le y \le y_m \\ h^3+3h^2(y_{m+1}-y)+3h(y_{m+1}-y)^2-3(y_{m+1}-y)^3 & y_m \le y \le y_{m+1} \\ (y_{m+2}-y)^3 & y_{m+1} \le y \le y_{m+2} \\ 0 & otherwise \end{cases} \qquad (2.9)$$

In spline finite strip analysis, every loaded cross-section of point force and every supported cross-section should coincide with some longitudinal knot in order to obtain satisfactory accuracy. Therefore, in some cases, unequal spacing between knots must be adopted. The unequally spaced B_3-spline $\varphi_m(y)$ with y_m as centre is given by:

$$\phi_m(y) = \begin{cases} 0 & y < y_{m-2} \\ f_1 & y_{m-2} \le y < y_{m-1} \\ f_2 & y_{m-1} \le y < y_m \\ f_3 & y_m \le y < y_{m-1} \\ f_4 & y_{m+1} \le y < y_{m+2} \\ 0 & y_{m+2} \le y \end{cases} \qquad (2.10)$$

where

$$
\begin{aligned}
f_1 &= \frac{(y-y_{m-2})^3}{(y_{m+1}-y_{m-2})\,(y_m-y_{m-2})\,(y_{m-1}-y_{m-2})} \\
f_2 &= f_1 - \frac{(y_{m+2}-y_{m-2})\,(y-y_{m-1})^3}{(y_{m+2}-y_{m-1})\,(y_{m+1}-y_{m-1})\,(y_m-y_{m-1})\,(y_{m-1}-y_{m-2})} \\
f_3 &= f_4 - \frac{(y_{m+2}-y_{m-2})\,(y_{m+1}-y)^3}{(y_{m+1}-y_{m-2})\,(y_{m+1}-y_{m-1})\,(y_{m+1}-y_m)\,(y_{m+2}-y_{m+1})} \\
f_4 &= \frac{(y_{m+2}-y)^3}{(y_{m+2}-y_{m-1})\,(y_{m+2}-y_m)\,(y_{m+2}-y_{m+1})}
\end{aligned}
\qquad (2.11)
$$

Thus, the spline finite strip method can easily be applied to problems with or without intermediate supports and with arbitrary loadings.

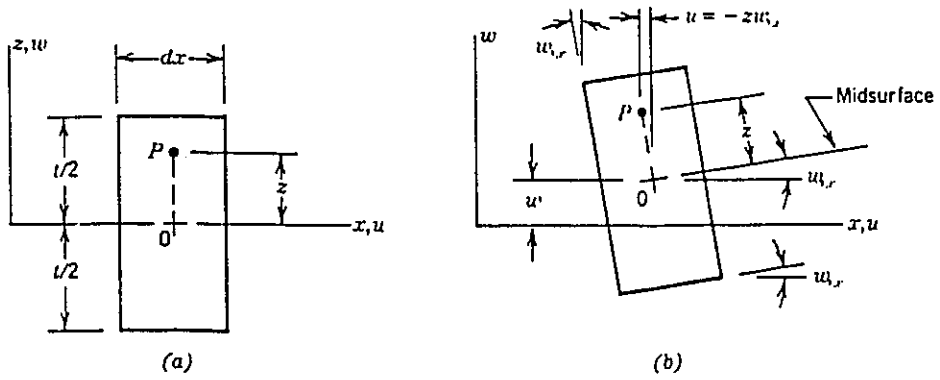

Figure 2.1. (a) Differential element of a thin plate before loading. (b) After loading: deformations associated with Kirchhoff plate theory. Point P displaces w units up and $zw_{,x}$ units leftward because of midsurface displacement w and small rotation $w_{,x}$.

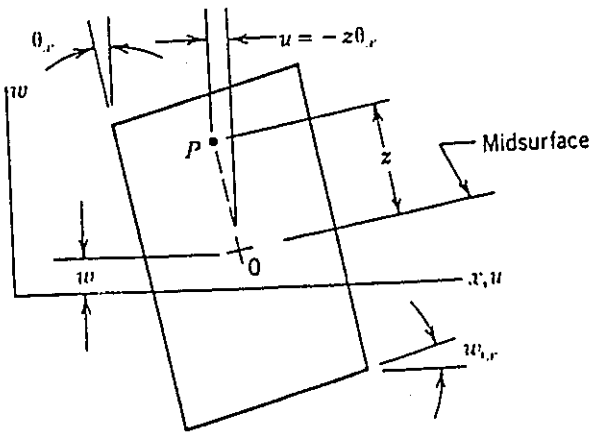

Fig.2.2.Differential plate element after loading, analogous to Fig.2.1.(b),but with transverse shear deformation allowed.

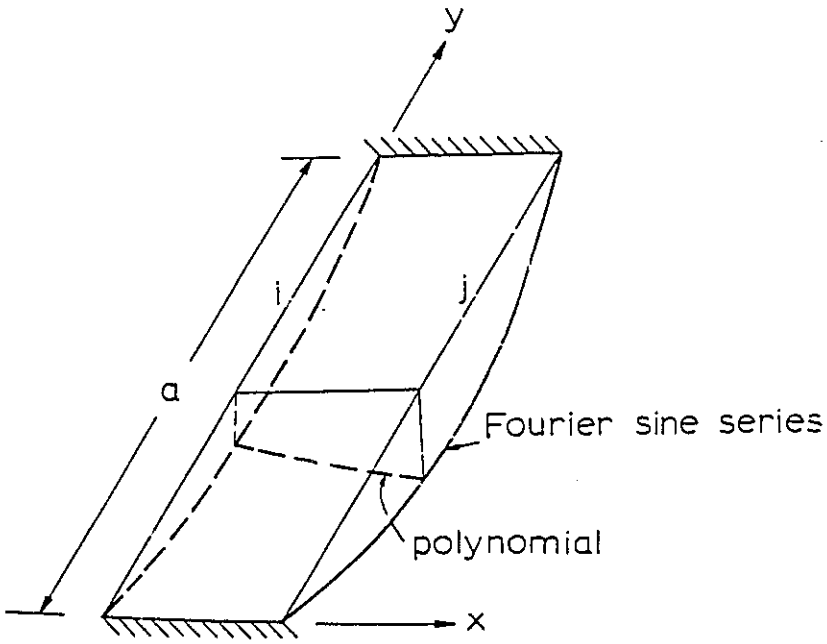

Figure.2.3. Typical finite strip for simple slab bridge.

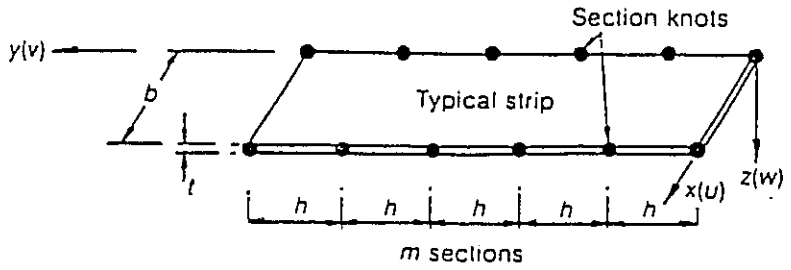

Fig.2.4.(a) Typical spline strip

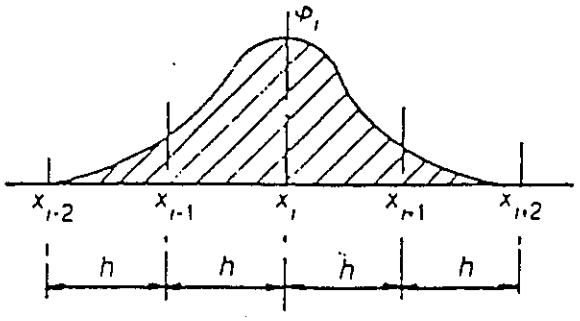

Fig.2.4.(b) Typical B_3-spline

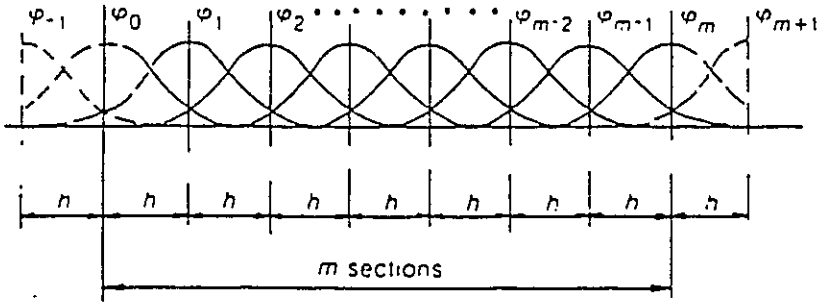

Figure.2.4.(c) Basis of B_3-spline expression

Chapter 3

Literature review

3.1. General

This chapter deals with a brief review of literature of the Mindlin plate theory and the spline finite strip method.

Research in the application of the thick finite strip is far less than that of the thin finite strip. In 1974, Mawenya and Davies [17] first introduced a thick plate strip for the solution of static problems and their work was extended by Benson and Hinton [18] to include vibration and stability applications for plates with one pair

of opposite edges simply supported. D.J.Dawe [19] developed four finite strip models for the flexural vibration analysis of rectangular plates with two opposite simply supported based on the Mindlin theory in 1978.

At approximately the same time, the finite strip method has been widely used to solve classical plate problems for plates of rectangular planforms and with general boundary conditions (i.e. with arbitrary combinations of simply supported, clamped and free edges) [20]. Because the finite strip method involves the assumption of a displacement field composed of products of the terms of an appropriate series in one coordinate direction (the longitudinal direction) and polynomial functions in the second (crosswise) coordinate direction, the longitudinal series must satisfy a priori the geometric boundary conditions at the plate ends. In the solution of classical plate problems the commonly used series for the deflection w are the fundamental mode shapes of uniform vibrating beams based on the Bernoulli-Euller theory (the one-dimensional equivalent of classical plate theory) and having appropriate end conditions. In attempting a finite strip analysis of thick rectangular plates using the Mindlin theory the approach is complicated by the necessity of selecting longitudinal series to represent each of the three reference quantities, w, θ_x and θ_y. The problem was overcome in 1980 by O.L.Roufaeil and D.J.Dawe [21], who introduced a relevant new longitudinal series effectively extending the finite strip method to successfully cover the general boundary conditions of the Mindlin plate. Later, the finite strip method was also extended to the geometrically nonlinear problem of rectangular

Mindlin plates by Z.G.Azizian and D.J.Dawe [36] in 1984.

All the research and resulting publications as mentioned above are restricted to the rectangular and the skewed plate only.

Since Y.K.Cheung and his colleagues published their new spline finite strip method in 1982, the numerical technique has been successfully applied to a wide variety of problems:

(i) the static and free vibration of rectangular plates in 1982 [10].

(ii) the static analysis of right box girder bridges in 1983 [22].

(iii) the analysis of skew plates in 1984 [40].

(iv) the vibration of irregular plates in 1984 [23].

(v) the analysis of curved slab bridge by plate theory in 1986 [2].

(vi) the analysis of general thin plates in 1986 [1].

(vii) the free vibration and static analysis of general plate in 1988 [24].

(viii) the free vibration analysis of arbitrarily doubly curved shell in 1989 [25].

(ix) the buckling analysis of arbitrarily shaped plates in 1990 [26].

However, the application of the method listed above has been limited to thin plate analysis. The object of the present study is to further extend the spline finite strip method to arbitrary shaped moderately thick plates using the Mindlin plate theory. A number of examples are presented in this thesis to demonstrate the

accuracy of the present method. From these numerical examples, it can be observed that the results given by the spline finite strip method compare favourably with those given by other numerical methods which are more laborious both in terms of computer time and data input.

Chapter 4

Analysis of arbitrary Mindlin plates

4.1. Introduction

The analysis of the arbitrary Mindlin plates may be carried out in three steps: coordinate transformation, discretization and numerical integration. The arbitrary-shaped bridge deck is first mapped into a square domain by suitable one to one transformation, and then discretization and analysis are carried out in the transformed plan, from which accurate results can be obtained for both thin and thick plates by using numerical integration.

4.2. Assembly of two coordinate transformations

In engineering structures, analysis of arbitrary shaped plates are often curved along two sides while the abutment/piers are skewed. Without loss of generality, a typical plan of such a plate can be represented in Cartesian co-ordinates as in Fig.4.1.

By making use of the cubic serendipity shape function, the plate can be mapped from the Cartesian co-ordinate system into the natural co-ordinate ξ-η plane, that is:

$$x = \sum_{i=1}^{8} N_i(\xi,\eta)\, x_i$$
$$y = \sum_{i=1}^{8} N_i(\xi,\eta)\, y_i \qquad (4.1)$$

where (x_i,y_i) are co-ordinates of the ith control point (node) on the curved edges of the plate, and $N_i(\xi,\eta)$ are the shape functions as given in table (4.1). Other mappings can also be used but it has been established that this simple cubic serendipity shape function is sufficiently accurate for most purposes.

Table 4.1. Shape function for simplified cubic serendipity element.

	$N_i(\xi,\eta)$
corner node (1,4,5,8)	$(1/32)(1+\xi_i\xi)\quad(9\eta^2-1)\quad(1+\eta^2\eta)$ $\xi_i=\pm1$ $\qquad\qquad$ $\eta_i=\pm1$
mid-side node (2,3,7,6)	$(9/32)(1+\xi_i\xi)\quad(1-\eta^2)\quad(1+9\eta_i\eta)$ $\xi_i=\pm1$ $\qquad\qquad$ $\eta_i=\pm1/3$

In the Mindlin plate theory, allowance is made for the effect of transverse shear deformation. Therefore, in addition to the lateral deflection which is the sole reference quantity of the classical plate theory, the two rotations about the in-plane plate axes also become independent reference quantities. Thus, the displacement field at any point of the plate can be expressed as:

$$\begin{aligned} u(x,y,z) &= -z\theta_x(x,y) \\ v(x,y,z) &= -z\theta_y(x,y) \\ w(x,y,z) &= w(x,y) \end{aligned} \qquad (4.2)$$

where u, v, and w are the displacements in the x, y, and z directions, respectively, and θ_x and θ_y are the rotations contained in the zx and yz planes, respectively. (see Figure 4.2).

The static analysis of the plate is defined by the equilibrium equation:

$$K\delta = F \qquad (4.3)$$

where K is the stiffness matrix of the plate, F is the external load vector, and δ is the displacement vector.

In order to formulate the stiffness and load matrices, it is necessary to obtain

the transformation between the first derivatives of θ_x, θ_y, w of the two co-ordinate systems.

According to the chain rule for derivatives,

$$\begin{bmatrix} \frac{\partial w}{\partial x} \\ \frac{\partial w}{\partial y} \end{bmatrix} = \begin{bmatrix} \frac{\partial \xi}{\partial x} & \frac{\partial \eta}{\partial x} \\ \frac{\partial \xi}{\partial y} & \frac{\partial \eta}{\partial y} \end{bmatrix} \begin{bmatrix} \frac{\partial w}{\partial \xi} \\ \frac{\partial w}{\partial \eta} \end{bmatrix} \tag{4.4}$$

Equation 4.4 is not directly available, but noting:

$$\begin{aligned} \frac{\partial w}{\partial \xi} &= \frac{\partial w}{\partial x} \cdot \frac{\partial x}{\partial \xi} + \frac{\partial w}{\partial y} \cdot \frac{\partial y}{\partial \xi} \\ \frac{\partial w}{\partial \eta} &= \frac{\partial w}{\partial x} \cdot \frac{\partial x}{\partial \eta} + \frac{\partial w}{\partial y} \cdot \frac{\partial y}{\partial \eta} \end{aligned} \tag{4.5}$$

and writing in matrix form:

$$\begin{bmatrix} \frac{\partial w}{\partial \xi} \\ \frac{\partial w}{\partial \eta} \end{bmatrix} = \begin{bmatrix} \frac{\partial x}{\partial \xi} & \frac{\partial y}{\partial \xi} \\ \frac{\partial x}{\partial \eta} & \frac{\partial y}{\partial \eta} \end{bmatrix} \begin{bmatrix} \frac{\partial w}{\partial x} \\ \frac{\partial w}{\partial y} \end{bmatrix} = [J] \begin{bmatrix} \frac{\partial w}{\partial x} \\ \frac{\partial w}{\partial y} \end{bmatrix} \tag{4.6}$$

where [J] is the so called Jacobian matrix.

From equation 4.1, we get:

$$[\,J\,] = \begin{bmatrix} \sum_{i=1}^{8} N_i(\xi,\eta)_{,\xi}\, x_i & \sum_{i=1}^{8} N_i(\xi,\eta)_{,\xi}\, y_i \\ \sum_{i=1}^{8} N_i(\xi,\eta)_{,\eta}\, x_i & \sum_{i=1}^{8} N_i(\xi,\eta)_{,\eta}\, y_i \end{bmatrix} \tag{4.7}$$

and matrix [Γ], the inverse matrix of [J] is given by:

$$[\Gamma] = [\,J\,]^{-1} = \frac{1}{|J|} \begin{bmatrix} J_{22} & -J_{12} \\ -J_{21} & J_{11} \end{bmatrix} = \begin{bmatrix} \Gamma_{11} & \Gamma_{12} \\ \Gamma_{21} & \Gamma_{22} \end{bmatrix} \tag{4.8}$$

where $|J|$ is the determinant of the Jacobian matrix:

$$|J| = \det[J] = J_{11}J_{22} - J_{21}J_{12}$$

Now we get the transformation between the first derivatives of the two co-ordinate systems as follows:

$$\begin{bmatrix} \frac{\partial}{\partial x} \\ \frac{\partial}{\partial y} \end{bmatrix} = \begin{bmatrix} \Gamma_{11} & \Gamma_{12} \\ \Gamma_{21} & \Gamma_{22} \end{bmatrix} \begin{bmatrix} \frac{\partial}{\partial \xi} \\ \frac{\partial}{\partial \eta} \end{bmatrix} \tag{4.9}$$

Subsequent manipulations are based on relations as stipulated by Eq.(4.9).

4.3. Finite strip formulation for the analysis of arbitrary Mindlin plates

The total potential energy of the plate can be written as [4]:

$$\pi = \frac{1}{2}\iint \varepsilon^T \sigma dxdy - \iint qwdxdy \qquad (4.10)$$

in which, for simplicity, only the contribution of the distributed load of intensity q(x,y) has been considered, ε and σ are respectively the generalized strain and stress vectors, which can be expressed as:

$$\varepsilon = [\varepsilon_b^T, \varepsilon_s^T]^T \qquad ; \qquad \sigma = [\sigma_b^T, \sigma_s^T]^T$$

By using Eq.(2.4) and Eq.(4.9), we can get the generalised stress and generalised strain in the transformed ξ-η coordinates as follows:

$$\sigma_b = \begin{Bmatrix} M_x \\ M_y \\ M_{xy} \end{Bmatrix} = \int_{-h/2}^{h/2} \begin{Bmatrix} \sigma_x \\ \sigma_y \\ \tau_{xy} \end{Bmatrix} z dz = [D_b] \begin{bmatrix} \dfrac{\partial \theta_x}{\partial x} \\ \dfrac{\partial \theta_y}{\partial y} \\ \dfrac{\partial \theta_x}{\partial y} + \dfrac{\partial \theta y}{\partial x} \end{bmatrix} = [D_b]\ [\Gamma_a] \begin{bmatrix} \dfrac{\partial \theta_x}{\partial \xi} \\ \dfrac{\partial \theta_x}{\partial \eta} \\ \dfrac{\partial \theta_y}{\partial \xi} \\ \dfrac{\partial \theta_y}{\partial y} \end{bmatrix} \qquad (4.11)$$

$$\sigma_s = \begin{Bmatrix} Q_x \\ Q_y \end{Bmatrix} = \int_{-h/2}^{h/2} \begin{Bmatrix} \tau_{xz} \\ \tau_{yz} \end{Bmatrix} dz = [D_s] \begin{bmatrix} \theta_x + \dfrac{\partial w}{\partial x} \\ \theta_y + \dfrac{\partial w}{\partial y} \end{bmatrix} = [D_s]\ [\Gamma_b] \begin{bmatrix} \theta_x \\ \theta_y \\ \dfrac{\partial w}{\partial \xi} \\ \dfrac{\partial w}{\partial \eta} \end{bmatrix} \qquad (4.12)$$

and

$$\varepsilon_b = \begin{bmatrix} \dfrac{\partial \theta_x}{\partial x} \\ \dfrac{\partial \theta_y}{\partial y} \\ \dfrac{\partial \theta_x}{\partial y} + \dfrac{\partial \theta_y}{\partial x} \end{bmatrix} = \begin{bmatrix} \Gamma_{11} & \Gamma_{12} & 0 & 0 \\ 0 & 0 & \Gamma_{21} & \Gamma_{22} \\ \Gamma_{21} & \Gamma_{22} & \Gamma_{11} & \Gamma_{12} \end{bmatrix} \begin{bmatrix} \dfrac{\partial \theta_x}{\partial \xi} \\ \dfrac{\partial \theta_x}{\partial \eta} \\ \dfrac{\partial \theta_y}{\partial \xi} \\ \dfrac{\partial \theta_y}{\partial \eta} \end{bmatrix} \qquad (4.13)$$

$$\varepsilon_s = \begin{bmatrix} \theta_x + \dfrac{\partial w}{\partial x} \\ \theta_y + \dfrac{\partial w}{\partial y} \end{bmatrix} = \begin{bmatrix} 1 & 0 & \Gamma_{11} & \Gamma_{12} \\ 0 & 1 & \Gamma_{21} & \Gamma_{22} \end{bmatrix} \begin{bmatrix} \theta_x \\ \theta_y \\ \dfrac{\partial w}{\partial \xi} \\ \dfrac{\partial w}{\partial \eta} \end{bmatrix} \qquad (4.14)$$

$$[\Gamma_a] = \begin{bmatrix} \Gamma_{11} & \Gamma_{12} & 0 & 0 \\ 0 & 0 & \Gamma_{21} & \Gamma_{22} \\ \Gamma_{21} & \Gamma_{22} & \Gamma_{11} & \Gamma_{12} \end{bmatrix} \qquad (4.15)$$

$$[\Gamma_b] = \begin{bmatrix} 1 & 0 & \Gamma_{11} & \Gamma_{12} \\ 0 & 1 & \Gamma_{21} & \Gamma_{22} \end{bmatrix} \tag{4.16}$$

with the sign convention for bending moments and shear forces shown in Figure 4.3, the relationship between the generalized stress and strains can be written as:

$$\sigma = D \cdot \varepsilon$$

and for an isotropic plate,

$$D = \begin{bmatrix} D_b & 0 \\ 0 & D_s \end{bmatrix} \tag{4.17}$$

where:

$$D_b = \frac{Eh^3}{12(1-\nu^2)} \begin{bmatrix} 1 & \nu & 0 \\ \nu & 1 & 0 \\ 0 & 0 & \frac{1-\nu}{2} \end{bmatrix} \tag{4.18}$$

$$D_s = \frac{\kappa Eh}{2(1+\nu)} \begin{bmatrix} 1 & 0 \\ 0 & 1 \end{bmatrix}$$

are respectively the bending and shear contributions to the elasticity matrix D; E and ν are the Young's modulus and Poisson's ratio respectively; h is the plate thickness and κ is a shear correction factor used to account for the warping of the section [38].

4.3.1 Displacement function

In the context of the spline finite strip, the whole domain Ω in ξ-η plane is partitioned into n strips along ξ-axis and m sections along η-axis, so that there are $n \times m$ subdomains and $3(m+3)(n+1)$ degrees-of-freedom for computation purposes (see Fig.4.4.). In strip j, the displacement can be expressed as:

$$F(\xi,\eta) = [N]\ [\Phi]\ \{\delta\}$$

where $F(\xi,\eta)=[\theta_x, \theta_y, w]$ is the displacement function, and N is the shape function. For linear, quadratic and cubic Mindlin plate strips, their shape functions are given in Fig.4.5, Φ is the spline function and δ is the displacement vector. For linear Mindlin spline strips, the displacements can be written as:

$$\theta_x(\xi,\eta) = [N_1, N_2]\begin{bmatrix}\Phi(\eta) & 0\\ 0 & \Phi(\eta)\end{bmatrix}\begin{Bmatrix}\{\theta_x\}_j\\ \{\theta_x\}_{j+1}\end{Bmatrix}$$

$$\theta_y(\xi,\eta) = [N_1, N_2]\begin{bmatrix}\Phi(\eta) & 0\\ 0 & \Phi(\eta)\end{bmatrix}\begin{Bmatrix}\{\theta_y\}_j\\ \{\theta_y\}_{j+1}\end{Bmatrix} \qquad (4.18)$$

$$w(\xi,\eta) = [N_1, N_2]\begin{bmatrix}\Phi(\eta) & 0\\ 0 & \Phi(\eta)\end{bmatrix}\begin{Bmatrix}\{w\}_j\\ \{w\}_{j+1}\end{Bmatrix}$$

where

$$N_1 = 1 - \bar{\xi}, \qquad N_2 = \bar{\xi}, \qquad \text{and} \qquad \bar{\xi} = \frac{(\xi - \xi_j)}{(\xi_{j+1} - \xi_j)} \tag{4.20}$$

$\{\theta_x\}_j$, $\{\theta_y\}_j$, and $\{w\}_j$ are vectors of rotation and deflections parameters along nodal line j. They are defined by:

$$\begin{aligned} \{\theta_x\}_j &= [\theta_{x_{j,-1}}, \theta_{x_{j,0}}, \ldots \theta_{x_{j,m}}, \theta_{x_{j,m+1}}]^T \\ \{\theta_y\}_j &= [\theta_{y_{j,-1}}, \theta_{y_{j,0}}, \ldots \theta_{y_{j,m}}, \theta_{y_{j,m+1}}]^T \\ \{w\}_j &= [w_{j,-1}, w_{j,0}, \ldots w_{j,m}, w_{j,m+1}]^T \end{aligned} \tag{4.21}$$

The spline functions for the whole strip can be represented by:

$$\Phi(\eta) = [\phi_{-1}(\eta), \phi_0(\eta), \ldots \phi_m(\eta), \phi_{m+1}(\eta)] \tag{4.22}$$

in which each local spline is given in Eq.(2.7).

In order to satisfy support conditions such as free, simple and clamped ends at the two ends of the plate, the local splines at the ends immediately adjacent to the boundary point have to be modified in accordance with Table (4.2). Another more convenient method of restraining the degrees of freedom by appropriate springs can be adopted to impose the general boundary condition and this will be discussed in more detail in the next Chapter.

Table 4.2. Modified local spline for end support

Boundary Condition	Modified local spline		
	φ_{-1}'	φ_0'	φ_1'
Free end	φ_{-1}	φ_0	φ_1
Simply supported end	Eliminated	$\varphi_0-4\varphi_{-1}$	$\varphi_1-\varphi_{-1}$
Clamped end	Eliminated	Eliminated	$\varphi_1-1/2\varphi_0+\varphi_{-1}$

4.3.2. Formulation of the stiffness matrix

Recalling Eq.4.11 and Eq.4.12, the bending strain of a Mindlin plate can be expressed as:

$$\{\varepsilon\}=\begin{bmatrix} \dfrac{\partial\theta_x}{\partial x} \\ \dfrac{\partial\theta_y}{\partial y} \\ \dfrac{\partial\theta_x}{\partial y}+\dfrac{\partial\theta_y}{\partial x} \\ \theta_x+\dfrac{\partial w}{\partial x} \\ \theta_y+\dfrac{\partial w}{\partial y} \end{bmatrix}_{5\times1} = \begin{bmatrix} \Gamma_a & 0 \\ 0 & \Gamma_b \end{bmatrix}_{5\times8} \begin{bmatrix} \dfrac{\partial\theta_x}{\partial\xi} \\ \dfrac{\partial\theta_x}{\partial\eta} \\ \dfrac{\partial\theta_y}{\partial\xi} \\ \dfrac{\partial\theta_y}{\partial\eta} \\ \theta_x \\ \theta_y \\ \dfrac{\partial w}{\partial\xi} \\ \dfrac{\partial w}{\partial\eta} \end{bmatrix}_{8\times1} \tag{4.23}$$

Combining with the displacement function, the strain-displacement relations

are given by:

$$\{\varepsilon\} = [\Gamma_T]\ [B]\ \{\delta\} \tag{4.24}$$

where

$$[B] = \begin{bmatrix}
N_1(\xi)_{,\xi}\cdot\phi(\eta) & 0 & 0 \\
N_1(\xi)\cdot\phi(\eta)_{,\eta} & 0 & 0 \\
0 & N_1(\xi)_{,\xi}\cdot\phi(\eta) & 0 \\
0 & N_1(\xi)\cdot\phi(\eta)_{,\eta} & 0 \\
N_1(\xi)\cdot\phi(\eta) & 0 & 0 \\
0 & N_1(\xi)\cdot\phi(\eta) & 0 \\
0 & 0 & N_1(\xi)_{,\xi}\cdot\phi(\eta) \\
0 & 0 & N_1(\xi)\cdot\phi(\eta)_{,\eta}
\end{bmatrix}$$

$$\begin{bmatrix}
N_2(\xi)_{,\xi}\cdot\phi(\eta) & 0 & 0 \\
N_2(\xi)\cdot\phi(\eta)_{,\eta} & 0 & 0 \\
0 & N_2(\xi)_{,\xi}\cdot\phi(\eta) & 0 \\
0 & N_2(\xi)\cdot\phi(\eta)_{,\eta} & 0 \\
N_2(\xi)\cdot\phi(\eta) & 0 & 0 \\
0 & N_2(\xi)\cdot\phi(\eta) & 0 \\
0 & 0 & N_2(\xi)_{,\xi}\cdot\phi(\eta) \\
0 & 0 & N_2(\xi)\cdot\phi(\eta)_{,\eta}
\end{bmatrix}_{8x6} \tag{4.25}$$

Eq.4.25 can be expanded to a 8×24 matrix for each section, since we know there are four splines related to one section.

Therefore, from the principle of the minimum potential energy, we get a system of linear equivalent equations,

$$\frac{\partial \pi}{\partial \delta_i} = 0 \qquad \rightarrow \qquad K\delta = F$$

where K is the overall stiffness matrix, and the stiffness matrix for one section is:

$$[K]_{24\times24} = \int\int [B]^T_{24\times8} [\Gamma]^T_{8\times5} [D]_{5\times5} [\Gamma]_{5\times8} [B]_{8\times24} |J| \, d\xi \, d\eta \qquad (4.26)$$

where J is the Jacobian matrix, and [D] is the property matrix as indicated in Eq.4.17. The integration is carried out section by section using the (2×2) Gaussian integration scheme. The overall stiffness matrix is obtained by summing up the contribution of each section. Further details of the numerical integration scheme will be discussed in the next Chapter.

Finally, the load vector can be obtained readily as in the standard finite element procedure as:

$$\{F\} = \int\int [\Phi]^T [N]^T \begin{Bmatrix} q \\ m_x \\ m_y \end{Bmatrix} |J| \, d\xi \, d\eta \qquad (4.27)$$

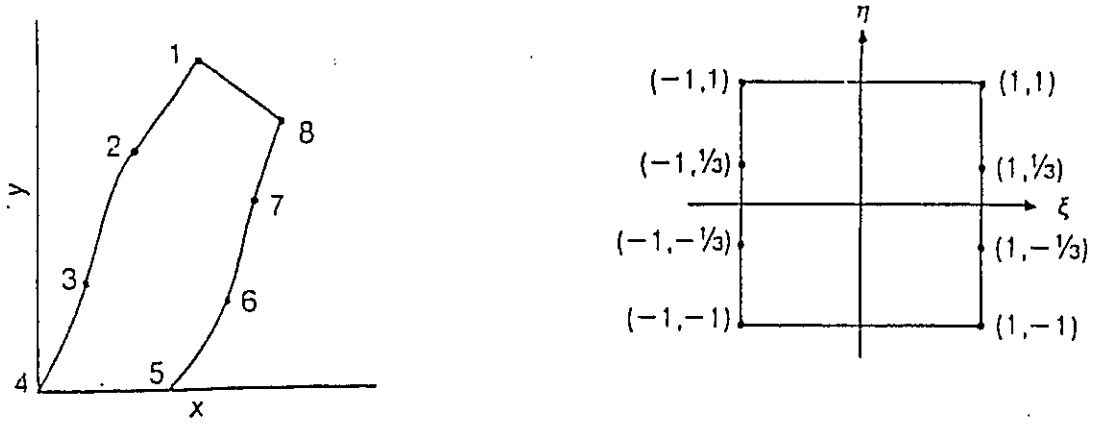

(a) typical plan of slab bridge.

(b) transformed domain for discretization.

Fig.4.1 Co-ordinate transformation

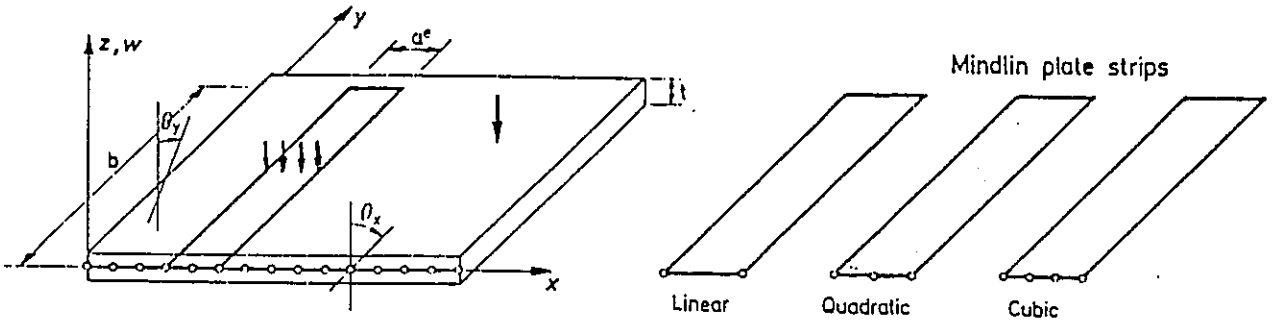

Fig.4.2. Typical Mindlin plate

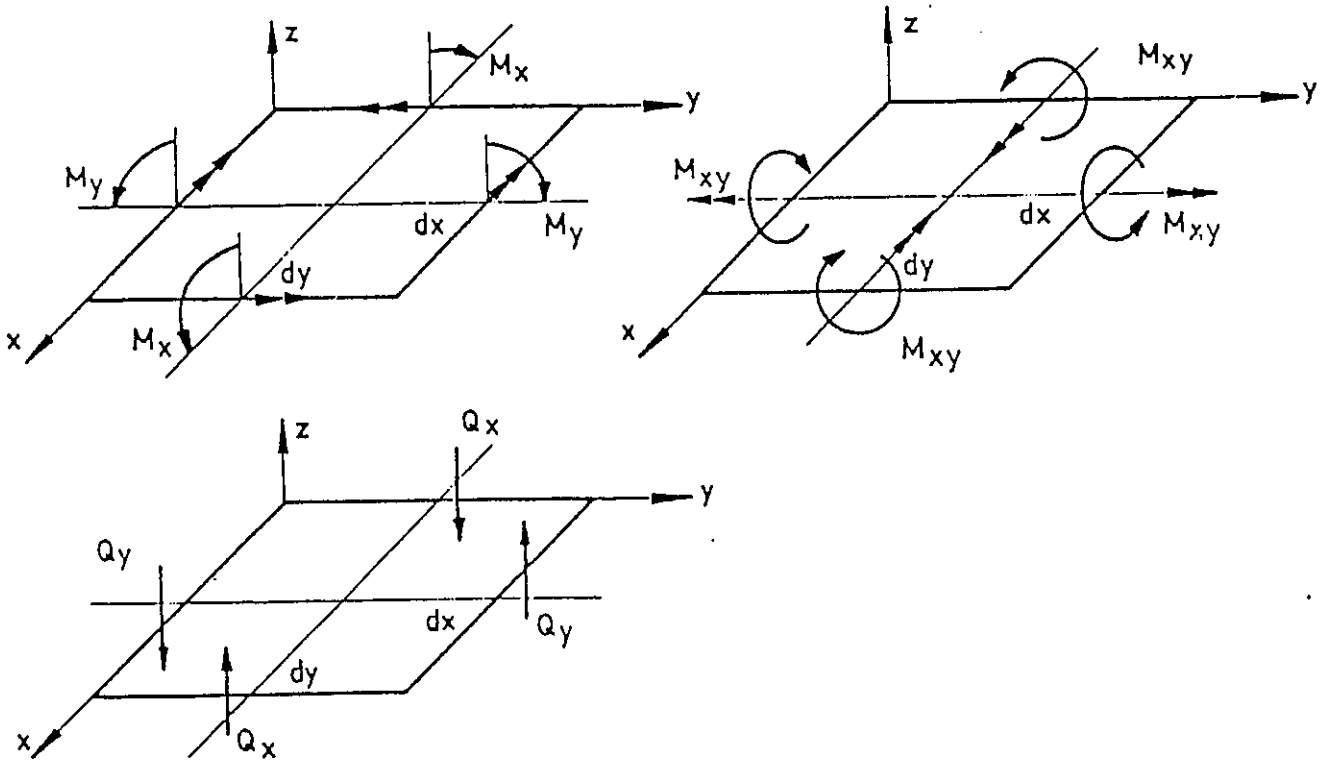

Fig.4.3 Sign convention for moments and shear forces

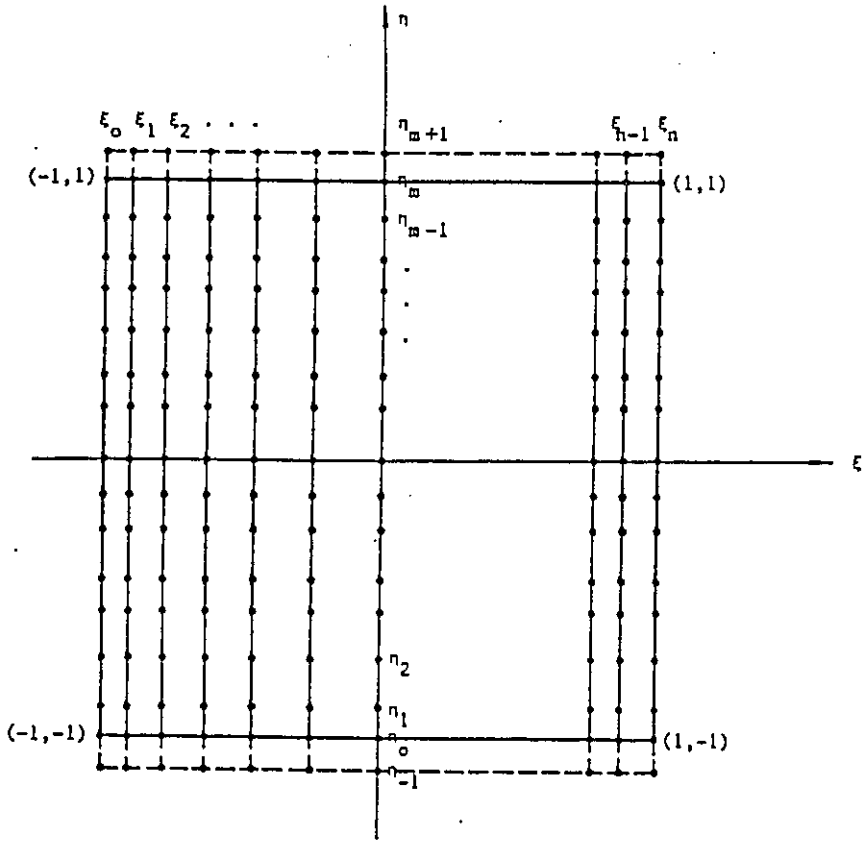

Fig.4.4. The discretisation of the transformed domain

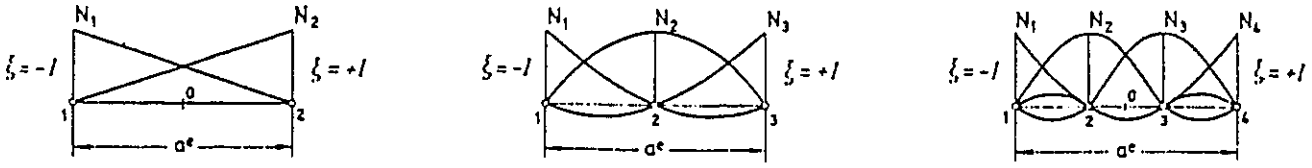

$$N_1 = \frac{1-\xi}{2}$$
$$N_2 = \frac{1+\xi}{2}$$
$$\xi = \frac{2(x-x_0)}{a^e}$$

$$N_1 = \frac{1}{2}\xi(\xi-1)$$
$$N_2 = (1-\xi)(1+\xi)$$
$$N_3 = \frac{1}{2}\xi(\xi+1)$$
$$\xi = \frac{2(x-x_2)}{a^e}$$

$$N_1 = -\frac{9}{16}\left(\xi^3 - \xi^2 - \frac{1}{9}\xi + \frac{1}{9}\right)$$
$$N_2 = \frac{27}{16}\left(\xi^3 - \frac{1}{3}\xi^2 - \xi + \frac{1}{3}\right)$$
$$N_3 = -\frac{27}{16}\left(\xi^3 + \frac{1}{3}\xi^2 - \xi - \frac{1}{3}\right)$$
$$N_4 = \frac{9}{16}\left(\xi^3 + \xi^2 - \frac{1}{9}\xi - \frac{1}{9}\right)$$
$$\xi = \frac{2(x-x_0)}{a^e}$$

Figure 4.5. Linear, Quadratic and Cubic Mindlin plate strips shape function

Chapter 5

Numerical Integration and Constraints

5.1. Numerical evaluation of the integrals

Numerical integration is widely used in the finite element method and the finite strip method. Apart from the 'full' numerical integration, the so called 'selective' and 'reduced' integration techniques [27,28,29] are also widely used in solving the 'shear locking' problem in recent years.

5.1.1 Quadrature rule and shear locking

Shear locking is a well known phenomenon for plates analyzed using a refined plate theory such as the Mindlin plate theory. The problem is similar to that experienced with Mindlin plate finite elements. As the plate thickness becomes small, the influence of the shear terms tends to dominate and the numerical solution may yield unrealistically overstiff results (locking) unless some precautions are taken. The use of deliberate under-integration in evaluating the stiffness properties of isoparametric plate elements, based on a shear deformation theory such as Mindlin plate theory, is now common practice. Before detailing the under-integration technique, we refer briefly in the next paragraph to the concept of Gauss quadrature.

'Quadrature' is the name applied to evaluating an integral numerically, rather than analytically as is done in tables of integrals. There are many quadrature rules. Here we discuss only the Gauss rules, as they are most appropriate for elements discussed in this thesis.

For the sake of brevity, let us take the one dimension problem as example, noting that the same method may be easily extended to two or three dimensional problems when required. An integral having arbitrary limits can be transformed so that its limits are from -1 to +1. With f=f(x), and with the substitution $x= 1/2(1-\xi)x_1 + 1/2(1+\xi)x_2$,

$$I=\int_{x_1}^{x_2} f\,dx \quad \rightarrow \quad I=\int_{-1}^{1} \phi\,d\xi \tag{5.1}$$

thus the integrand is changed from f=f(x) to $\phi=\phi(\xi)$, where ϕ incorporates the Jacobian of the transformation. The latter form of Eq.(5.1) makes it possible to write the convenient quadrature formulas as,

$$\int_{-1}^{+1} \phi(\xi)\,d\xi = \sum_{i=1}^{n} W_i f(\xi_i) \tag{5.2}$$

Thus, instead of doing integration, we evaluate $\phi=\phi(\xi)$ at each of several locations ξ_i to obtain ordinates ϕ_i, multiply each ϕ_i by an appropriate weight W_i, and add. A polynomial of degree 2n-1 is integrated exactly by n-point Gauss quadrature. Use of more than n points will still produce the exact result. We consider the n-point Gauss quadrature as the 'full' numerical integration. If the function $\phi=\phi(\xi)$ is not a polynomial, Gauss quadrature is inexact, but becomes more accurate as more points are used. Table 5.1 shows the data of sampling points and weights.

The foregoing linear transformation is sufficient to make arbitrary limit changes. We can always consider a convenient reference interval such as -1 to +1. In practice the limit change is done automatically by isoparametric transformation.

Table 5.1. Sampling points and weights for Gauss quadrature over the interval ξ=-1 to ξ=+1.

Order n	Location ξ_i of Sampling Point	Weight Factor W_i
1	0	2
2	± 0.57735 02691 89626	1
3	± 0.77495 66692 41482	0.55555 55555 55555
	0	0.88888 88888 88888

5.1.2. The selective and reduced integration for Mindlin finite strips

The earliest work on this topic was by Zienkiewicz, Taylor, and Too [27] and the so-called reduced integration technique was proposed to tackle the locking difficulty. The method was conceived as a 'trick' in the beginning in earlier applications. It was not until a few years later that a heuristic explanation was provided with the clear observation that the stiffening of the structure was due to shear locking. When using 'full' Gaussian numerical integration for the element based on the shear deformation theory such as the Mindlin plate theory, efficient performance with accurate results are obtained for thick plates and shells but results obtained are excessively stiff for plates with thin geometry; reduction in the order of numerical integration leads to considerable improvement in accuracy for thin plates,

whether such reduction is 'selective' or 'reduced'. Regarding the terminology used here, 'full' integration (n × n points over the element middle surface) means an order of integration sufficient to calculate the stiffness matrix exactly for a rectangular or parallelogrammic-shaped element; 'selective' integration implies the use of (n-1) × (n-1) integration points in evaluating the transverse shear stiffness contribution and n × n points in evaluating all other contributions; and 'reduced' integration implies the use of (n-1) × (n-1) points in evaluating all stiffness contributions. One can regard the stiffness matrix of a Mindlin plate element as being composed of a bending stiffness $[k_b]$ and a transverse shear stiffness $[k_s]$. From Equation 4.25 with $[B] = [B_b] + [B_s]$, we get:

$$[k] = \int_A [B_b]^T [D_M] [B_b] \, dA + \int_A [B_s]^T [D_M] [B_s] \, dA \qquad (5.3)$$

where, $[B_b]$ is associated with in-plane strains ε_x, ε_y, and γ_{xy} and is obtained by setting rows 4 and 5 of [B] to zero. $[B_s]$ is associated with transverse shear strains γ_{yz} and γ_{zx}, and is obtained by setting rows 1, 2, and 3 of [B] to zero. Cross product terms $[B_b]^T[D_M][B_s]$ and $[B_s]^T[D_M][B_b]$ are zero because of the distribution of zero in $[B_b]$, $[B_s]$ and $[D_M]$. Bending stiffness $[k_b]$ mobilizes only the $[D_K]$ portion of $[D_M]$, and transverse shear stiffness $[k_s]$ mobilizes only the $G_{yz}t$ and $G_{zx}t$ terms in $[D_M]$.

Each integration point used for $[k_s]$ brings two constraints to a Mindlin plate

element, one associated with γ_{yz} and the other with γ_{zx}. Locking of the Mindlin plate element caused by too many transverse shear constraints can be avoided by adopting a reduced or selective integration rule to generate [k] [39].

The number of integrating points required to exactly integrate the strip matrices obviously depends on the degree of the shape function polynomials of each particular strip. Table 5.2 gives the number of Gaussian integrating points needed for the full, reduced and selective integration of k_b and k_s.

Table 5.2. Gaussian integration rules for matrices k_b and k_s for various Mindlin strip element.

Strip Element	Gaussian Number of integration points					
	Full(F)		Selective(S)		Reduced(R)	
	k_b	k_s	k_b	k_s	k_b	k_s
Linear	2	2	2	1	1	1
Quadratic	3	3	3	2	2	2
Cubic	4	4	3	3	3	3

5.2. Penalty function method

A number of methods for imposing boundary conditions have been proposed by

Cheung et al [1,2,10]. In this thesis, the penalty function method is chosen to treat end and intermediate support conditions of the strips.

As an example, it is assumed that the displacement component W at point(x,y) is prescribed to be zero, that is:

$$w=\sum_m N_m(x,y)\, w_m=0$$

where $N_m(x,y)$ and w_m are associated displacement functions and displacement parameters respectively.

In order to impose this constraint in the analysis, a fictitious spring with large stiffness α might be introduced in the corresponding direction at the point(x,y). Its strain energy or penalty function is:

$$U=\frac{1}{2}\alpha w^2=\frac{1}{2}\alpha\sum_m\sum_n N_m(x,y)\, N_n(x,y)\, w_m w_n$$

From this expression it can be seen that the stiffness matrix of this imaginary spring is:

$$[k_{mn}] = [\alpha N_m(x, y)\, N_n(x, y)]$$

If the first derivative of deflection, say $w_{,y}$, at point(x,y) is prescribed to be zero, then

$$\frac{\partial w}{\partial y} = \sum_m \frac{\partial N_m(x, y)}{\partial y} w_m = 0$$

Following the same procedure, the required stiffness matrix for this constraint can be obtained as:

$$[k_{mn}] = [\alpha \frac{\partial N_m(x, y)}{\partial y} \frac{\partial N_n(x, y)}{\partial y}]$$

It should be mentioned that the spring stiffness will affect the node in question and two adjacent nodes in the B_3-spline finite strip method. Assembling the stiffness matrices of all point constraints with the structural stiffness matrix will accomplish the treatment of boundary conditions. For example, if the displacement w is prescribed to be zero at node i, then the stiffness matrix must be modified by adding the new stiffness:

$$
[K] = \alpha \begin{array}{c} \\ i-1 \\ i \\ i+1 \end{array}
\begin{array}{c}
\begin{array}{ccc} i-1 & i & i+1 \end{array} \\
\begin{bmatrix} 1 & 4 & 1 \\ 4 & 16 & 4 \\ 1 & 4 & 1 \end{bmatrix}
\end{array}
$$

Assembling the stiffness of all point constraints to the structural stiffness matrix will complete the treatment of the boundary.

Any elastic support can also be included by the same method, as long as the spring stiffness α can actually represent the stiffness of this support.

The choice of α should be made after one has chosen an integration rule that avoids ill conditional matrix of the mesh. The numerical behaviour of the penalty function method was investigated by Carlos A. Felippa [35], and a 'moderately large' number (10^3-10^5) (if we think the biggest datum in the stiffness matrix is 1) was suggested, in order to avoid numerical difficulty associated with these constraints, the choice of α should be taken with great care.

Chapter 6

Numerical examples

6.1. Example 1--Square plates

Square plates are used as a typical case to demonstrate the accuracy and versatility of the numerical method presented. Here, two mesh sizes (6×6 and 8×8) of the spline finite strip are used to deal with the problem.

The displacement at the centre of the plate under uniform load q or point load P can be written respectively as:

$$w=\alpha\frac{qL^4}{Eh^3} \qquad and \qquad w=\beta\frac{PL^2}{D}$$

where, h is the plate thickness, L is the length of the plate, E is the Young's modulus $D=Eh^3/12(1-\nu^2)$ is the flexural rigidity of the plate, and ν is the Poisson's ratio.

For different ratios of plate thickness to length and with different boundary conditions, the results for centre deflection are listed in Tables 6.1-6.4. For the sake of comparison, results obtained by other researchers are also listed in the same tables.

Table 6.1 Simply supported square plate under uniform load

	α				
h/L	6 × 6	8 × 8	Thin plate theory [34]	Thick plate theory [30]	Mindlin plate FEM [31]
0.01	0.04433*	0.04460*	0.04434	0.04439	0.04470
0.10	0.04526	0.04631	0.04434	0.04632	0.04689
0.15	0.04589	0.04856	0.04434	-------	0.04977
0.20	0.05158	0.05258	0.04434	0.05217	0.05384
0.25	0.05766	0.05830	0.04434	-------	0.05900
0.30	0.06458	0.06499	0.04434	0.06192	0.06536

*: reduced integration method used.

Table 6.2 Simply supported square plate under point load

	β			
h/L	6 × 6	8 × 8	Mindlin plate FEM [31]	FEM** (4X6)
0.01	0.01016*	0.01179*	0.01173	0.01157
0.10	0.01139	0.01300	0.01350	0.01294
0.15	0.01477	0.01625	0.01579	0.01584
0.20	0.01852	0.02011	0.01900	0.01875
0.25	0.02300	0.02487	0.02313	--------
0.30	0.02833	0.03059	0.02817	--------

*: reduced integration method used.

Table 6.3. Clamped square plate under uniform load

	α			
h/L	6 × 6	8 × 8	Mindlin plate FEM [31]	FEM** (4X6)
0.01	0.01358*	0.01385*	0.01403	0.01369
0.10	0.01455	0.01553	0.01654	0.01566
0.15	0.01764	0.01845	0.01952	0.01847
0.20	0.02264	0.02315	0.02375	0.02288
0.25	0.02843	0.02877	0.02895	-------
0.30	0.03527	0.03544	0.03543	-------

*: reduced integration method used.

**: 8-node isoparametric thick plate element [39].

Table 6.4 Clamped square plate under point load

	β			
h/L	6 × 6	8 × 8	Mindlin plate FEM [31]	FEM** (4X6)
0.01	0.00524*	0.00559*	0.00575	0.00555
0.10	0.00680	0.00729	0.00757	0.00702
0.15	0.00995	0.01015	0.00990	0.00968
0.20	0.01317	0.01369	0.01314	0.001312
0.25	0.01719	0.01802	0.01730	--------
0.30	0.02157	0.02365	0.02236	--------

*: reduced integration method used.

**: 8-node isoparametric thick plate element [39].

From table 6.1, we can see that Timoshenko's results (using the classical thin plate theory) are only valid for very thin plates such as h/L=0.01. From the table, it is evident that Timoshenko's results would be unacceptable even for moderately thick plates (h/L≥0.15). Table 6.1 to Table 6.4 demonstrate the accuracy and versatility of the present spline finite strip method very well in that with very simple data input, results agree well with other researches who used much more cumbersome thick plate theory [30] or the extensive data input as required by the Mindlin plate finite element method [31].

6.2. Example 2--Fan shaped bridge deck

Since the main objective of this thesis is to extend the spline finite strip method to the analysis of arbitrary shaped thick plates or bridge decks, it is the purpose here to apply the method to a relatively thick curved bridge deck. A 60° fan-shaped thin bridge deck (Fig.6.1) is first analyzed. The arbitrary thin fan-shaped deck has internal and external radii of 177.8 mm (7 in) and 330.2 mm (13 in) respectively, the Young's modulus and Poisson's ratio are 460000 lbf/in^2 (6239.4 MPa) and 0.35 respectively; the original thickness of the plate is 4.267 mm (0.168 in). Two additional deck thicknesses of 6.807 mm (0.268 in) and 22.047 mm (0.868 in) are also used here in order to demonstrate that the spline finite strip method presented here can solve accurately both thin and moderately thick arbitrary shaped plates or bridge decks. The bridge was simply supported along its two ends. Concentrated loads were applied at three different locations (Points A, B and C), and the mid-span deflections resulting from these loadings were tabulated in Table 6.5 to Table 6.7, and compared with Cheung [25] (thin plate theory spline finite strip method), coull [32] (thin plate theory finite element method), Sawko [33] (a real experiment and thin plate theory finite element method) and W.C.Li [41] (8-node isoparametric thick plate element). Good agreements are found throughout. The distributions of the tangential moment across the mid-span (thickness = 0.168 in) were also plotted in Fig.6.2. A computer program previously used by W.C.Li [41] based on the Mindlin plate theory using an 8-node isoparametric thick plate element [39] was used for comparison purposes for the two additional thicknesses. It should be emphasized that although the finite element method can successfully deal with the same problems as the present method,

it is demonstrated here that the present method is far simplier in that much less data preparation and computer time are required to yield the same degree of accuracy. In Appendix B, the input data file for both the finite element method (mesh size 4x6) and the spline finite strip method (mesh size 8x8) are listed. As can be observed, the data preparation for the finite element method contains tedious input even for the 8-node isoparametric element used. Further, strictly speaking, in order to arrive at the same continuity condition and accuracy as the cubic spline function presented (C_2 continuity), a 12-node isoparamatric element should have been used resulting in a further increase of the data input requirements of approximal 30 percent or more.

6.3 Example 3--Fan shaped continuous isotropic bridge deck

One of the most important advantages of spline finite strip method in comparison with the original finite strip method is that the spline finite strip method can treat bridge decks with arbitrary intermediate supports and arbitrary point loads. A fan shaped continuous isotropic deck originally designed and tested by F.Sawko and P.A.Merriman in 1971 is used here to demonstrate this particular versatility of the spline finite strip method presented. Details of this model are shown in Fig.6.3. The 60° fan-shaped model was point-supported at eight points by columns which offered only vertical restraint along four radial lines. Point load was applied at two different locations (Point A and B), and the mid-span deflections and moments

resulting from these loadings were compared with those from Sawko [33] in Fig.6.4 to Fig.6.7. It is evident from these figures that results of the spline finite strip method presented here compare extremely well with the result obtained by Sawko and Merriman [33].

Table 6.5. Deflections across mid-span of fan-shaped plates

(plate thickness=0.268 in)

loading case	Radius (in)	Present Method* (8X8)	FEM** (4X6)
Point loading at A	13.0	0.02217	0.02223
	11.5	0.01624	0.01624
	10.0	0.01143	0.01144
	8.5	0.00762	0.00766
	7.0	0.00465	0.00475
Point loading at B	13.0	0.01143	0.01144
	11.5	0.00919	0.00918
	10.5	0.00725	0.00724
	8.5	0.00535	0.00534
	7.0	0.00378	0.00378
Point loading at C	13.0	0.00465	0.00475
	11.5	0.00410	0.00414
	10.0	0.00378	0.00378
	8.5	0.00378	0.00375
	7.0	0.00433	0.00424

*: reduced integration method used.

**: 8-node isoparametric thick plate element [39].

Table 6.6. Deflections across mid-span of fan-shaped plates

(plate thickness=0.868 in)

loading case	Radius (in)	Present Method (8X8)	FEM** (4X6)
Point loading at A	13.0	0.0006823	0.0006881
	11.5	0.0004981	0.0004969
	10.0	0.0003474	0.0003471
	8.5	0.0002248	0.0002283
	7.0	0.0001239	0.0001344
Point loading at B	13.0	0.0003474	0.0003471
	11.5	0.0002800	0.0002786
	10.5	0.0002219	0.0002204
	8.5	0.0001603	0.0001600
	7.0	0.0001088	0.0001108
Point loading at C	13.0	0.0001239	0.0001344
	11.5	0.0001132	0.0001191
	10.0	0.0001088	0.0001108
	8.5	0.0001136	0.0001142
	7.0	0.0001373	0.0001405

**: 8-node isoparametric thick plate element [39].

Table 6.7. Deflections across mid-span of fan-shaped plates

(plate thickness=0.168 in)

Loading case	Radius (in)	Coull[32]	Y.K.Cheung Tham and Li	*Present Method (8X8)	Sawko[33]
Point loading at A	13	0.0876	0.08821	0.08867	0.0888
	11.5			0.06515	
	11	0.0578	0.05794		0.0582
	10			0.04237	
	9	0.0353	0.03543		0.0355
	8.5			0.03086	
	7	0.0194	0.01948	0.01913	0.0198
Point loading at B	13	0.0457	0.04578	0.04599	0.0459
	11.5			0.03704	
	11	0.0342	0.03428		0.0344
	10			0.02924	
	9	0.0241	0.02414		0.0241
	8.5			0.02168	
	7	0.0155	0.01554	0.01541	0.0154
Point loading at C	13	0.0195	0.01948	0.01913	0.0194
	11.5			0.01680	
	11	0.0163	0.01634		0.0163
	10			0.01541	
	9	0.0157	0.01523		0.0150
	8.5			0.01530	
	7	0.0169	0.01705	0.01732	0.0168

*: reduced integration method used.

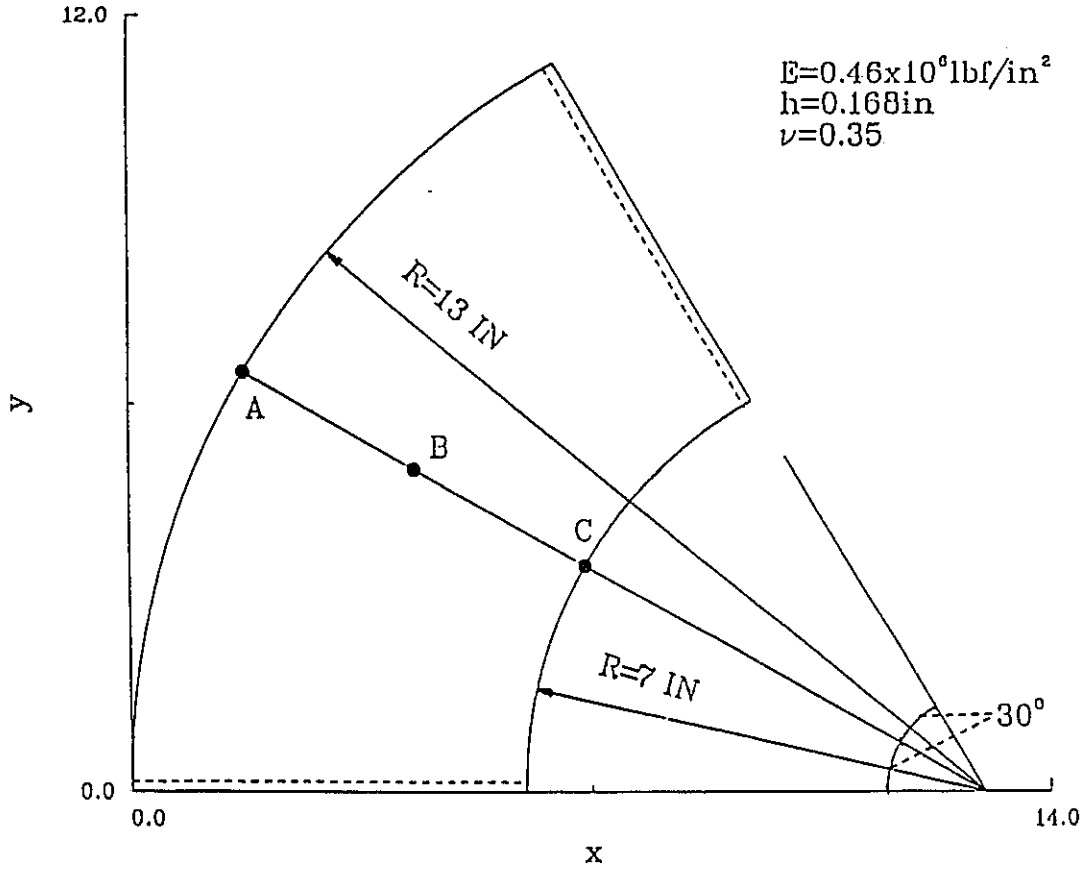

Figure 6.1 Fan-shaped bridge deck model (example 2)

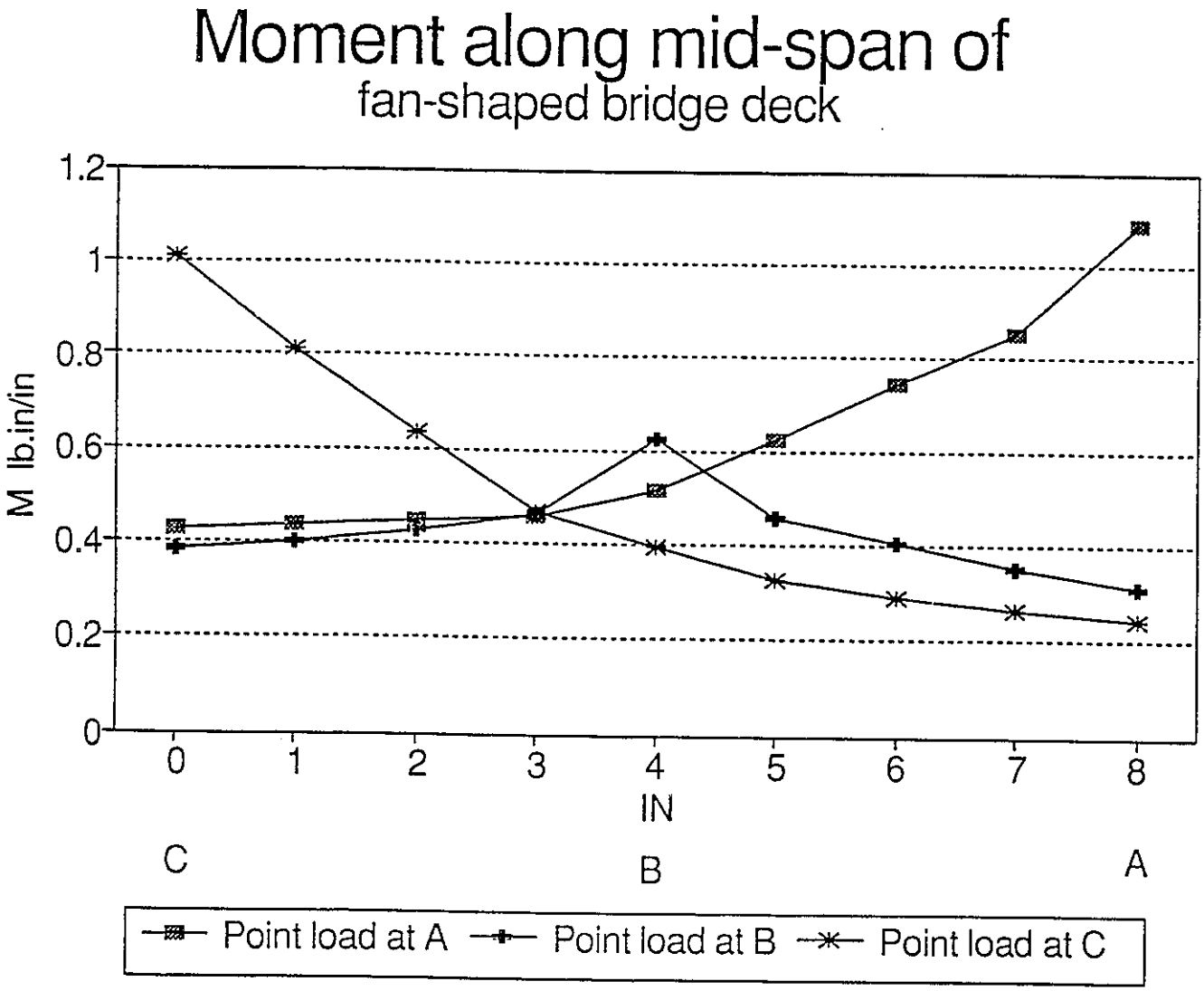

Figure 6.2 Moments along mid-span of fan-shaped bridge deck

(thickness = 0.168 in)

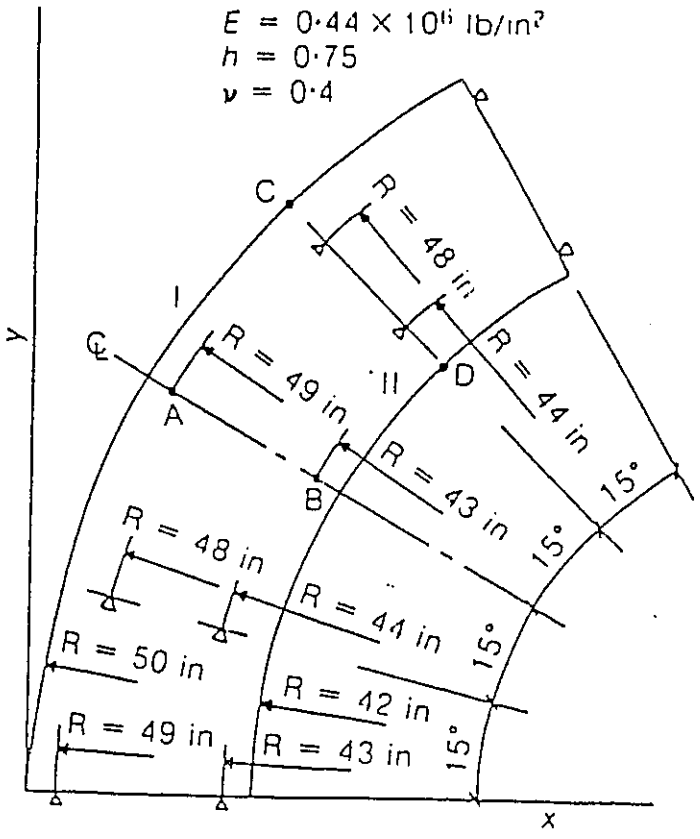

Figure 6.3 Fan-shaped continuous bridge model (example 3)

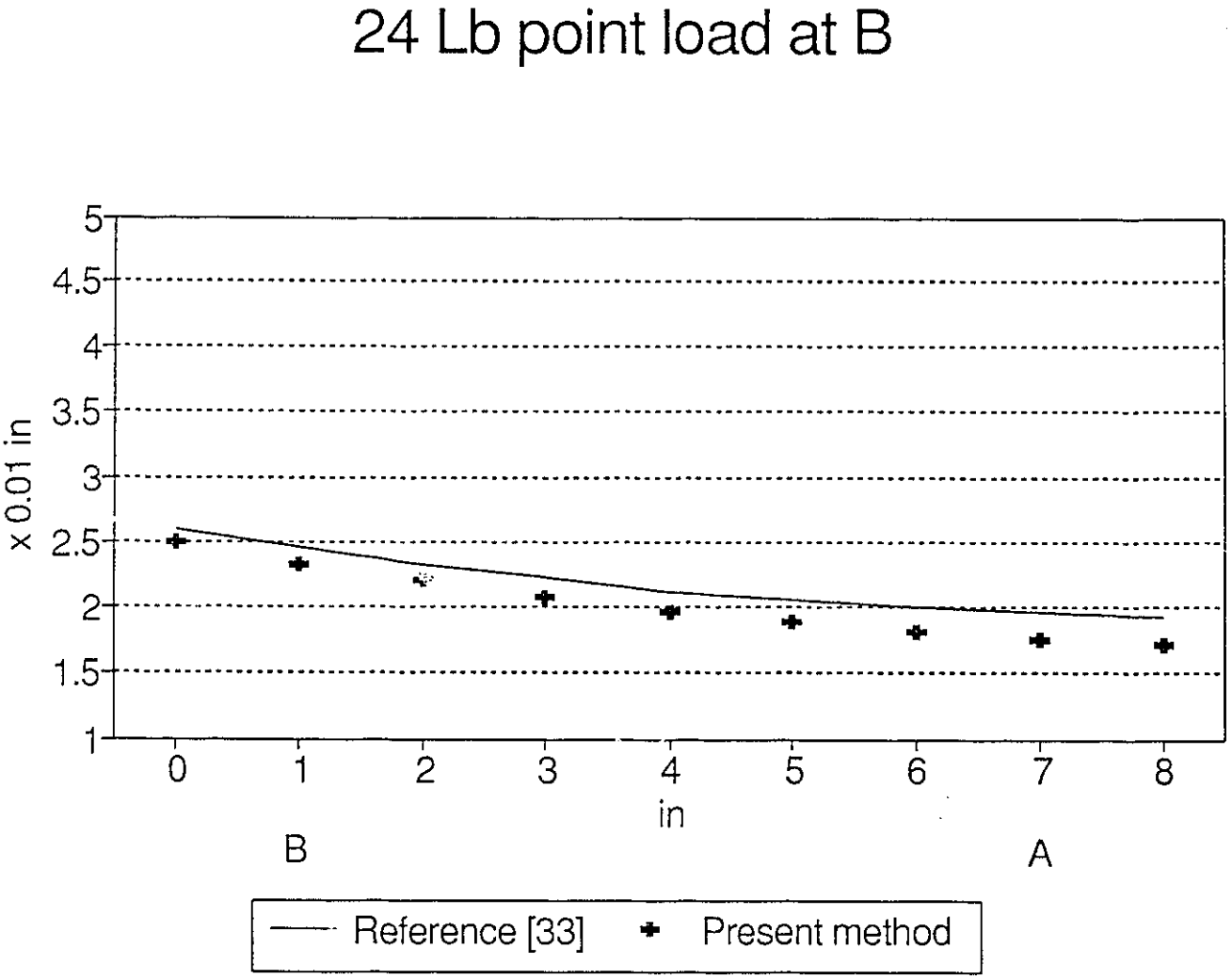

Figure 6.4.1 Transverse deflection across symmetrical line AB (1)

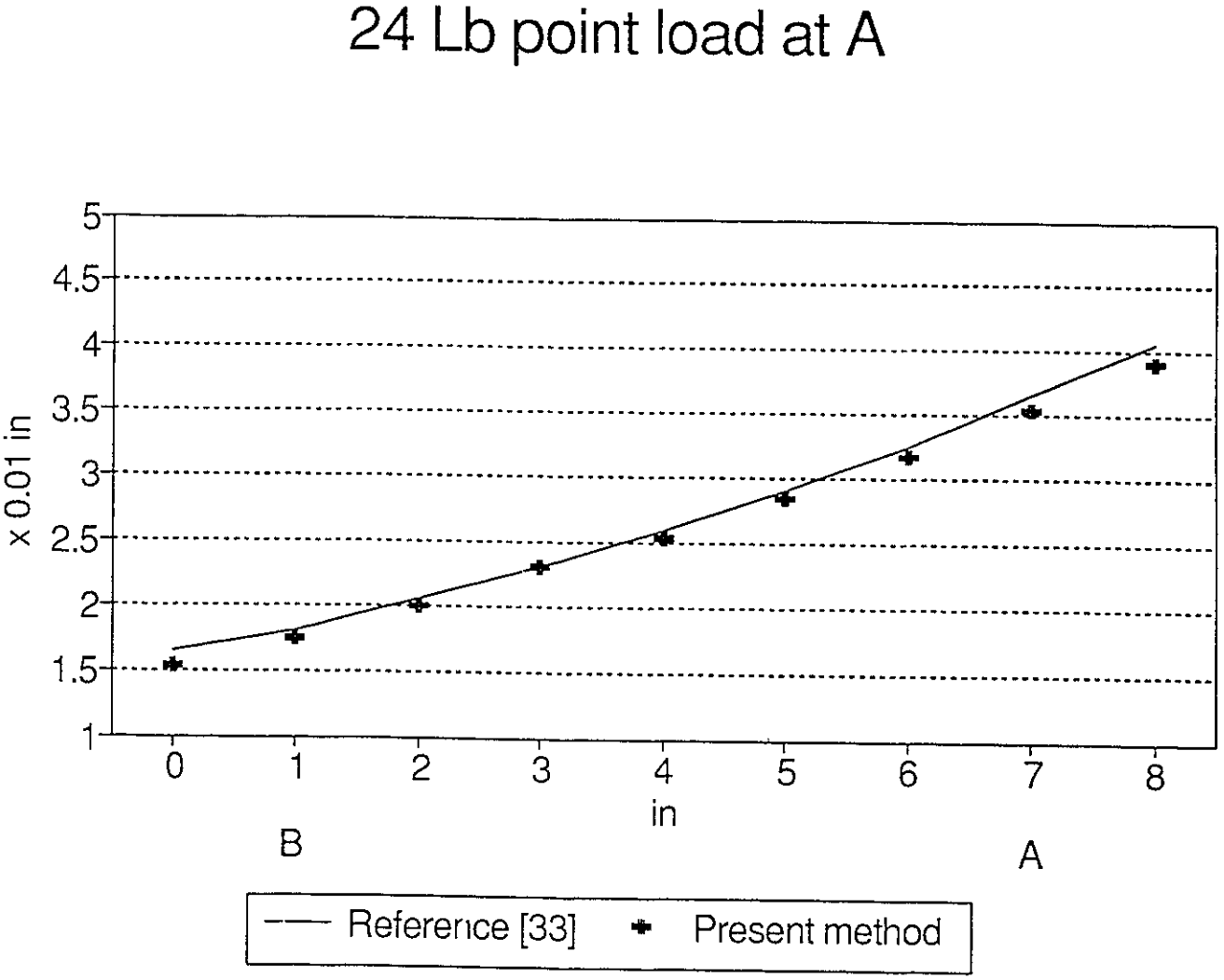

Figure 6.4.2 Transverse deflection across symmetrical line AB (2)

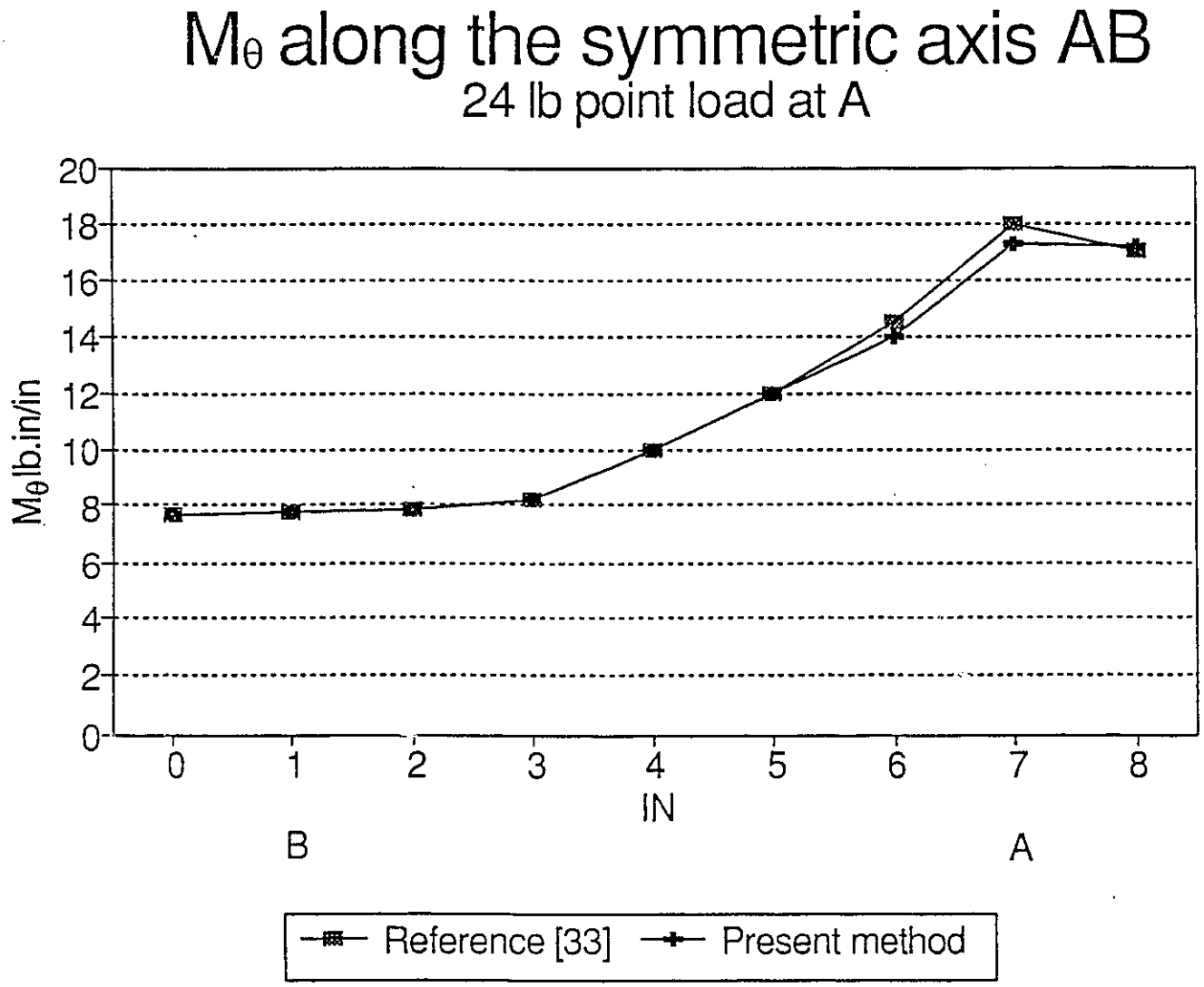

Figure 6.5 Longitudinal moment (M_θ) along the symmetric axis AB (1)

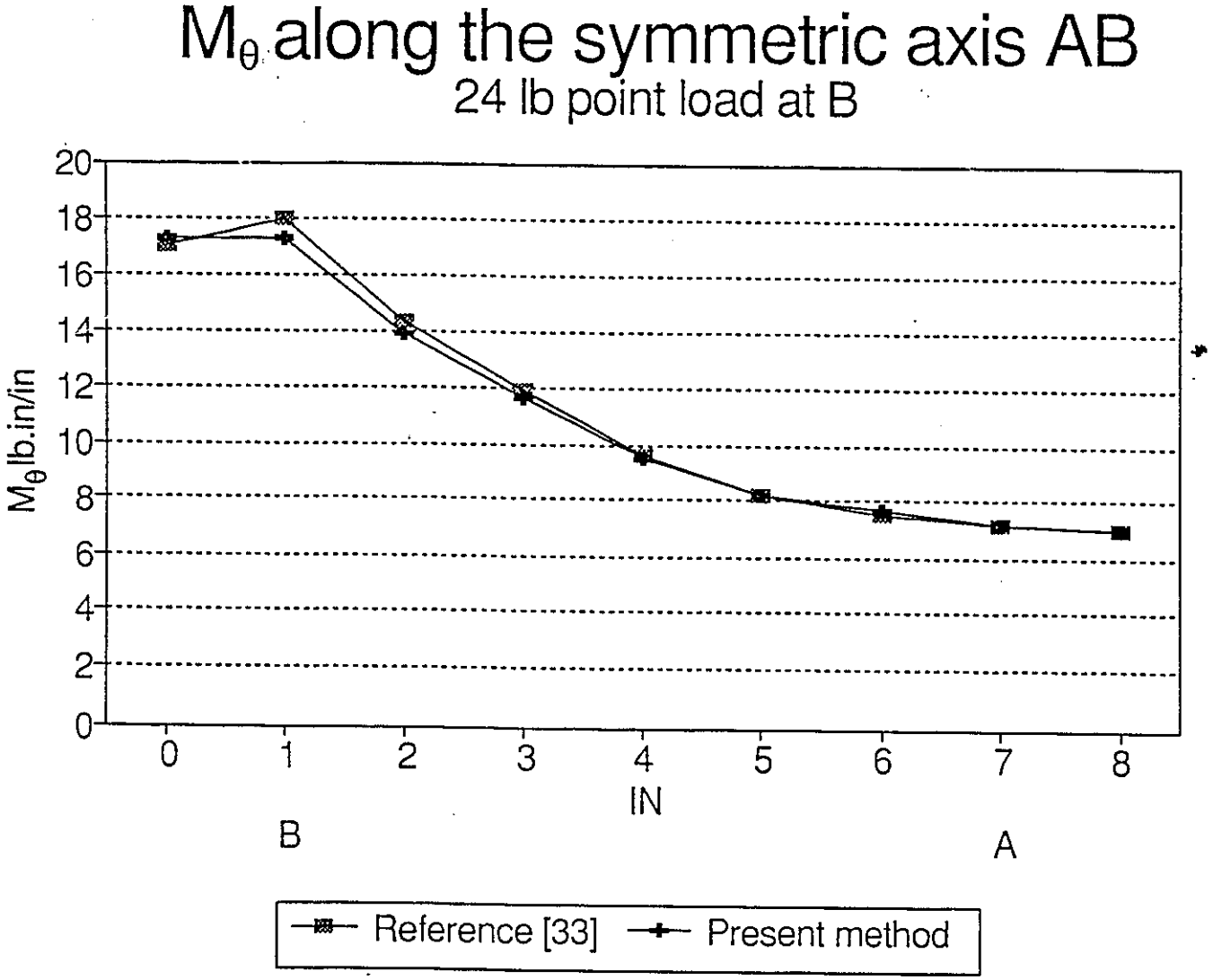

Figure 6.6 Longitudinal moment (M_θ) along the symmetric axis AB (2)

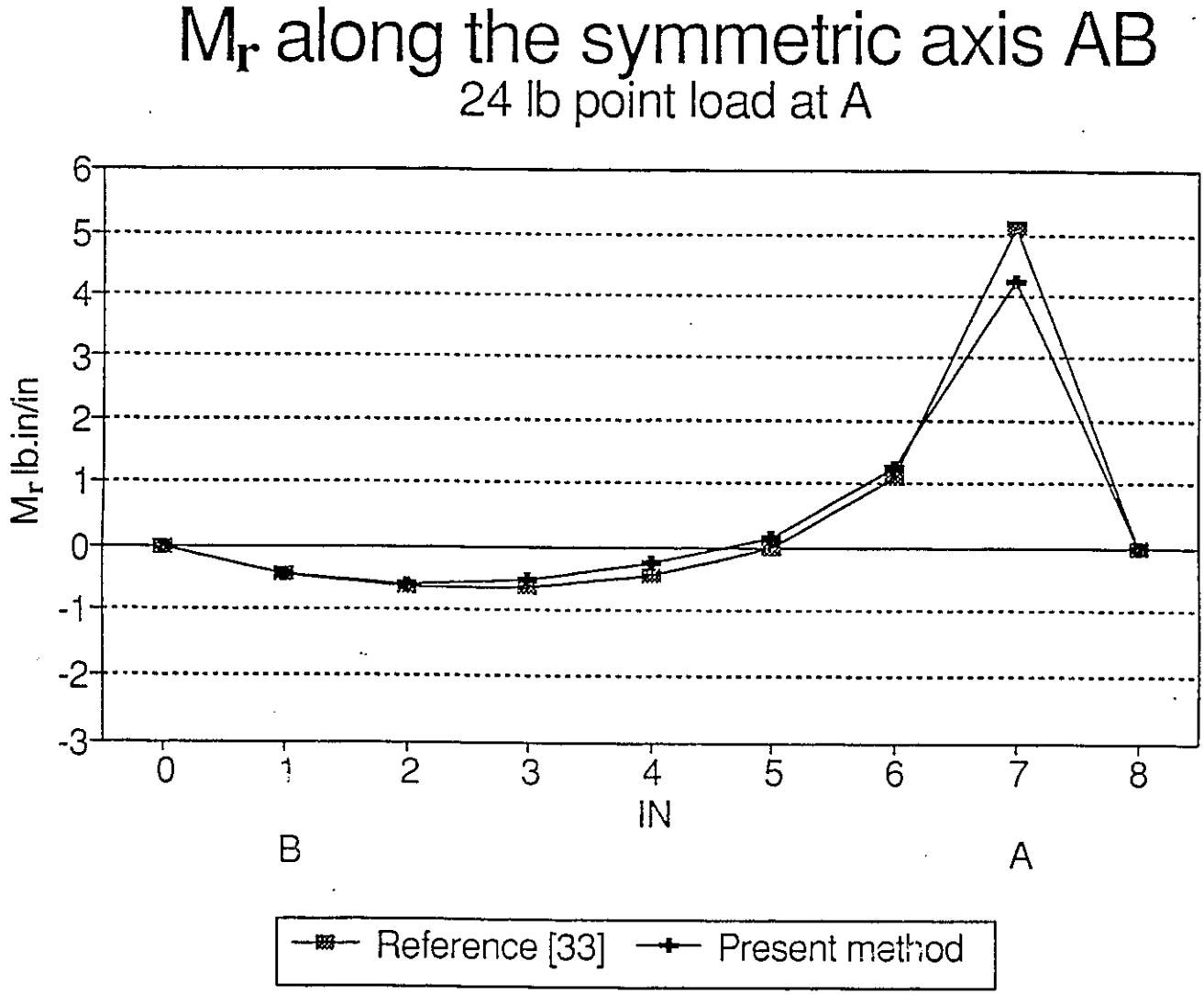

Figure 6.7 Transverse moment (M_r) along the symmetric axis AB

6.4. Example 4--Fully clamped elliptical plate

Consider an elliptical plate as shown in Fig.6.8. The plate is fully clamped and subjected to a uniform load q. For various aspect ratios of a/b, the deflection and bending moment at the centre of the plate is listed in table 6.8. Excellent agreements are obtained with results recently obtained by Liew [42].

Table 6.8 Fully clamped elliptical plate under uniform load

		a/b = 1.0	a/b = 1.5	a/b = 2.0
$wD/(qa^4)$	Present method (8x8)	0.000983	0.000348	0.000137
	Ritz functions [42]	0.000977	0.000344	0.000132
$M_x/(qa^2)$	Present method (8x8)	0.020190	0.007104	0.002717
	Ritz functions [42]	0.020310	0.007162	0.002754
$M_y/(qb^2)$	Present method (8x8)	0.020221	0.007134	0.002736
	Ritz functions [42]	0.020310	0.007162	0.002754

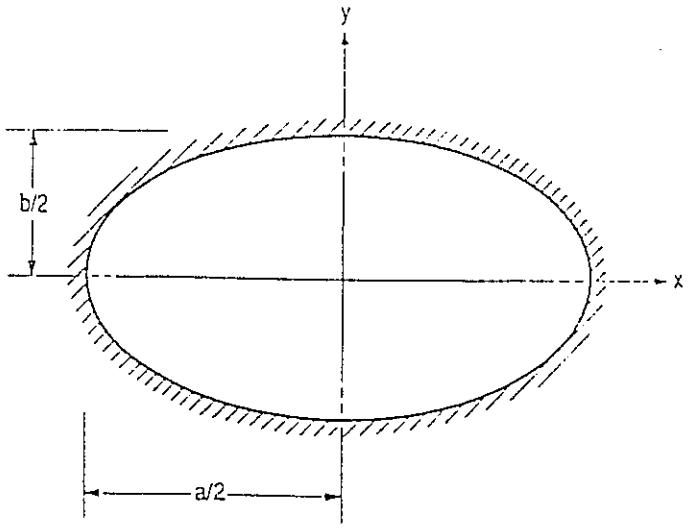

Figure 6.8 Fully clamped elliptical plate

Chapter 7

Discussions and conclusions

7.1. Discussion

In the development of the finite element method and finite strip method, continuity is a major problem with regard to application and convergence. The spline finite strip method as presented in this thesis can now overcome this problem, with the B_3 spline functions ensuring continuity up to the second derivative (the so-called C_2 continuity). By comparison, in order to achieve the same continuity condition, the finite element method needs three times as many unknowns at the element nodes. Hence, when C_2 continuity is required, the use of B_3 splines is computationally much

more efficient than the finite element method.

The second derivative of B_3 spline varies linearly in each longitudinal section, with the result that it can more readily simulate peak values of bending moment at the loaded cross-section or at an intermediate support.

Another advantage of spline finite strip method is that it can easily take up any prescribed external boundary condition, by using the penalty function approach. Thus, the spline strip method is more flexible than the semi-analytical finite strip method in imposing boundary conditions.

When applied to arbitrary shaped plates, the reduction in data input is significant by using the spline finite strip method presented in comparison with the use of the finite element method, with a corresponding significant reduction in computer time. For the fan-shaped bridge deck used as an example in this thesis, the data input as required by the spline strip method is less than 15 percent of that required by the finite element method. The list of data input required is shown in Appendix B.

A further advantage of the present method lies in its capacity to deal with moderately thick plates or bridge slabs overcoming the deficiencies of the conventional classical thin plate approach of analysis.

7.2. Conclusions

A spline finite strip method to analyze moderately thick plates and bridge decks of arbitrary shapes according to Mindlin plate theory is developed in this thesis. The reduced integration technique is used to eliminate 'shear locking', and the penalty function method is utilized to impose boundary condition at the end of strips and intermediate supports. Numerical examples have demonstrated that:

1. The spline finite strip method presented here can be applied successfully to analyze moderately thick plates of length-to-thickness ratio from 0.01 to 0.30.

2. The present method yields very accurate results for both thin and moderately thick rectangular and arbitrary shaped bridge decks subjected to both uniform and concentrated loads, and is believed to be much more efficient than the conventional finite element method both in terms of data input and computation time required.

3. The method successfully overcomes the deficiencies of the conventional finite strip method in the treatment of arbitrary boundaries, patch loadings or intermediate supports. Further, the input data required is less than those generally required by the conventional finite element method.

7.3. Recommendation for further research

The following recommendations are made for future research:

1. Further research is needed to extend the spline finite strip method to cover the analysis of arbitrary shaped moderately thick bridge decks with material and geometric nonlinearitis, and the vibration analysis of arbitrary shaped Mindlin plates.

2. Further investigation should also be made to the 'under integration method' with the view to provide a better understanding to the shear locking problem of thin plates using the Mindlin plate theory.

References

1. W.Y.Li, Y.K.Cheung and L.G.Tham, Spline Finite Strip Analysis of General Plates. Journal of Engineering Mechanics, Vol.112, No.1, January, 1986, pp.43-54.

2. Y.K.Cheung, L.G.Tham and W.Y.Li, Application of spline-finite-strip method in the analysis of curved slab bridge. Proc.Instn Civ.Engers, Part 2,1986,81, pp.111-124.

3. R.D.Mindlin, Influence of Rotatory Inertia and Shear on Flexural Motions of Isotropic Elastic Plates. Journal of applied mechanics, 37, 1951, pp.1031-1036.

4. S.Timoshenko and S.Woinowsky-Krieger, Theory of plates and shells, 2nd edition McGraw-Hill, New York, 1959.

5. E.Reissner, The Effect of Transverse Shear Deformation on the Bending of Elastic Plates. Journal of applied mechanics, 12, 1945, pp.69-77.

6. E.Reissner, On bending of elastic plates. Quarterly of applied mathematics, 5, 1947, pp.55-68.

7. H.Hencky, Uber die Berucksi.'ıtigung der Schubverzerrungen in ebenen Platten. Ingenieur ahchive, 16, 1947, pp.7?-76.

8. A.Kromm, Verallgemeinerte Theorie der Plattenstatik. Ingenieur archive, 21, 1953, pp.266-286.

9. A.Kromm, Über die Randquerkräfte bei gestützten platten. Zeitschrift fuer Angewandte Mathematik und Mechanik, 35, 1955, pp.231-242.

10. Y.K.Cheung, S.C.Fan, C.Q.Wu, Spline Finite Strip in structure analysis,

Proceedings, the international conference on finite element method, Shanghai, 1982, pp.704-709.

11. I.J.Schoenberg, Contributions to the problem of approximation of equidistant data by analytic functions. Quarterly of applied mathematics, 4, 1946, pp.45-99 and pp.112-114.

12. J.H.Ahlberg, E.M.Nilson and J.L.Walsh, The theory of spline and their applications. Academic Press, New York,1967.

13. T.N.E.Greville, Theory and applications of spline functions. Academic Press,New York, 1969.

14. M.H.Schultz, Spline analysis. Prentice-Hall, New Jersey,1973.

15. G.Birkhoff and C.R.de Boor, Piecewise polynomial interpolation and approximation. In 'Approximation of functions' (ed.H.L.Garabedian), Elsevier,Amsterdam,1965, pp.164-190.

16. P.M.Prenter, Splines and variational methods. John Wiley, New York,1975.

17. A.S.Mawenya and J.D.Davies, Finite strip analysis of plate bending including transverse shear effects. Building Science, 1974, 9, pp.175-180.

18. P.R.Benson and E.Hinton, A thick finite strip solution for static , free vibration and stability problems. International Journal of Numerical Methods in Engineering , 1976, 10, pp.665-678.

19. D.J.Dawe, Finite strip models for vibration of Mindlin plates. Journal of Sound and Vibration, 1978,59(3), pp.441-452.

20. Y.K.Cheung, Finite Strip Method in Structural Analysis. Pergamon press,

Oxford (1976).

21. O.L.Roufaeil and D.J.Dawe, Vibration analysis of rectangular Mindlin plates by the finite strip method. Computer & Structures, Vol 12,1980, pp.833-842.

22. Y.K.Cheung, S.C.Fan, Static analysis of right box girder bridges by spline finite strip method. Proc.Instn Civ.Engrs, Part2, 1983,75, June, pp.311-323.

23. J.L.Chen and K.P.Chong, Vibration of irregular plates by finite strip method with splined functions. Engineering Mechanics in Civil Engineering, Proc. of the 5th Engineering Mechanics Div., ASCE (Edited by A.P.Boresi and K.P.Chong), Vol.1. pp.256-260 (1984).

24. Y.K.Cheung, L.G.Tham and W.Y.Li, Free vibration and static analysis of general plate by spline finite strip. Computational Mechanics, 1988, 3, pp.187-197.

25. Y.K.Cheung, L.G.Tham and W.Y.Li, Free vibration analysis of arbitrarily doubly curved shell by spline finite strip method. Research Report, University of Hong Kong (1989).

26. L.G.Tham and H.Y.Szeto, Buckling analysis of arbitrarily shaped plates by spline finite strip method. Computer & Structures, Vol.36.No.4.1990, pp.729-735.

27. O.C.Zienkiewicz, R.L.Taylor, J.M.Too, Reduced integration technique in general analysis of plates and shells. Int. J. Numer.Meth.Engng, 3,1971, pp.275-290.

28. T.J.R.Hughes, M.Cohen and M.Haoun, Reduced and selecetive integration techniques in the finite element analysis of plates. Nucl. Engng Des. 46, 203 (1978).

29. O.C.Zienkiewicz and E.Hinton, Reduced integration, function smoothing and non-conformity in finite element analysis (with special reference to thick plates).

J.Franklin Inst.302, 1976, pp.443-461.

30. V.L.Salerno & M.A.Goldberg, Effect of shear deformations on the bending of rectangular plates. Journal of applied mechanics, Vol.27, No.1,1960, pp 54-58.

31. Generalised conforming finite element and its applications in structure engineering, J.Q.Zhou, Ph.D thesis, Qinghua University, 1989.

32. Coull A. and Das P.C., Analysis of curved bridge decks. Proc.Instn Civ.Engrs. 1967, 37, May, pp.75-85.

33. Sawko F. and Merriman P.A. Finite element analysis of bridge curved in plan. Developments in bridge design and construction. Crosby LockWood & Son Ltd. 1971, pp.334-236.

34. S.Timoshenko and W.Krieger, Theory of Plates and Shells, 2th edition, Mcgraw-Hill Book company, 1959.

35. Carlos A. Felippa, Inerative procedures for improving penalty function solutions of algebraic systems. International journal for numerical methods in engineering, Vol. 12, 1978, pp.821-836.

36. Z.G.Azizian and D.J.Daew, Geometrically non-linear analysis of rectangular Mindlin plates using the finite strip method. Computers & Structures, 21, 1985, pp.423-436.

37. Y.K. Cheung, The finite strip method in the analysis of elastic plates with two opposite simply supported ends. Proc.Instn Civ.Engrs., vol.40, Dec. 1968, pp.1-7.

38. S.Timoshenko, Strength of Materials, Van Nostrand, New York, 1955.

39. R.D.Cook, D.S.Malkus, M.E.Plesha, Concepts and applications of finite element

analysis, 3th edition, John Wiley & Sons, 1989.

40. M.J.Chen, L.G.Tham,Y.K.Cheung, Spline finite strip for parallelogram plate. Conf. on Accuracy Estimates and Adaptive Refinements in Finite Element Computations, Lisbon, Portugal, 1984, Vol. 1, pp. 19-22, 95-104.

41. W.C.Li, privation communications.

42. K.M.Liew, Response of plates of arbitrary shape subject to static loading. Journal of Engineering Mechanics, Vol. 118, No. 9, September, 1992. pp. 1783-1794.

Appendix A

```
C=====================================================================
C
C       ARRAY NAME              DESCRIPTION
C
C
C    ELCOD(2,8)          X AND Y COORDINATE FROM CURVED EDGES
C                       1= X , 2= Y
C    XINEL, ATMEL          XI AND ETA COORDINATES FOR EACH STRIPS
C                    NODE LINE
C    MAPSP(8)             A SHAPE FUNCTION USED FOR MAPPING
C    GUMM                 JACOBIAN MATRIX
C    FORMA                FORCE MATRIX
C    DISMA               DISPLACEMENT MATRIX
C    STIFF               ELEMENT STIFFNESS MATRIX
C    SSTIF               STRUCTURAL STIFFNESS MATRIX
C
C=====================================================================

      IMPLICIT REAL*8(A-H,O-Z)
      DIMENSION ELCOD(2,8)
      DIMENSION SSTIF(400,400),FORMA(400,1)
      DIMENSION DMAT(5,5)
      DIMENSION DISMA(400,1), BOUND(3,3)
      DIMENSION THETAX(81)   ,THETAY(81)  ,W(81)

C
C  ===================================================
C
C     PROGRAM FOR THE ANALYSIS OF ARBITRARY PLATES
C         BY THE MINDLIN FINITE STRIP METHOD.
C
C  ===================================================
C


C
C     FIRST, CALL INPUT TO READ ALL DATA
C

      CALL INPUT(ELCOD,THICK,NELEM,MELEM,YOUNG,POISS)
```

```
C
C     COMPUTER THE PLATE STIFFNESS MATRIX
C

      CALL STIFP(NELEM,MELEM,SSTIF,ELCOD,THICK,YOUNG,POISS,
     , DMAT,NDF,WI,HI)
C
C     CITE THE BOUNDARY CONDITION
C

      CALL SBOUND(BOUND,SSTIF,NDF)
C
C     INVENSION STIFFNESS MATRIX
C

      CALL MATIN(SSTIF,NDF)

C
C     MAKING FORCE MATRIX
C

      READ(5,*) NF,MF,SF,NFTYPE
      GO TO (1,2) NFTYPE
    1 CALL FORCE(297,NF,MF,SF,FORMA)
      GOTO 3
    2 CALL FUNIF(297,WI,HI,FORMA,NELEM,MELEM,ELCOD)
      GOTO 3
    3 CALL MATMUL(SSTIF,297,297,FORMA,1,DISMA)

C
C     USE SPLINE FUNCTION TO CALCULATE THE REAL DISPLACEMENT
C

      CALL DEFORM(DISMA,THETAX,THETAY,W)

C
C     BENDING MOMENT AND SHEAR FORCE CALCULATION
C

      CALL BENDMO(DISMA,ELCOD,NELEM,MELEM,HI,WI,DMAT)
```

```
      STOP
      END

C
C
C     SUBROUTINES
C
C


      SUBROUTINE INPUT(ELCOD,THICK,NELEM,MELEM,YOUNG,POISS)
      IMPLICIT REAL*8(A-H,O-Z)
      DIMENSION ELCOD(2,8)
      DO 300 I=1,2
      READ (5,*)  (ELCOD(I,J),J=1,8)
      WRITE(6,52)  (ELCOD(I,J),J=1,8)
   52 FORMAT(8F10.5,/)
  300 CONTINUE
      READ(5,*) THICK,NELEM,MELEM
      READ(5,*) YOUNG,POISS
      NDF=3*(NELEM+1)*(MELEM+3)
      WRITE(6,545) YOUNG, POISS,THICK,NELEM,MELEM
  545 FORMAT(2X,F12.5,2X,F8.3,2X,F8.4,2X,I2,2X,I2,/)
      RETURN
      END


      SUBROUTINE STIFP(NELEM,MELEM,SSTIF,ELCOD,THICK
     , ,YOUNG,POISS,DMAT,NDF,WI,HI)
      IMPLICIT REAL*8(A-H,O-Z)
      DIMENSION ELCOD(2,8)
      DIMENSION SSTIF(NDF,NDF)
      DIMENSION STIFF(24,24) ,DMAT(5,5)

      WI=2.0/NELEM
      HI=2.0/MELEM
      NDF=3*(NELEM+1)*(MELEM+3)
C
C
      DO 179  II=1,NDF
```

```
      DO 179  JJ=1,NDF
  179 SSTIF(II,JJ) = 0.0D0

C
C     LOOP OVER EACH ELEMENT
C

      DO 80  IELEM = 1,NELEM
      DO 81  JELEM = 1,MELEM
      XINEL = -1.0 + WI*(IELEM -1)
      ATMEL = -1.0 + HI*(JELEM -1)

C
C     CALCULATE ELEMENT STIFFNESS MATRIX
C

      CALL ELMSTI(WI,HI,IELEM,JELEM,STIFF,ELCOD,THICK,YOUNG,POISS
     , ,DMAT,XINEL,ATMEL,NELEM,MELEM)

C
C     ADD THE ELEMENT STIFFNESS MATRIX INTO GLOBE STIFFNESS MATRIX
C

  321 CALL LOGIC(MELEM,IELEM,JELEM,STIFF,SSTIF)
   81 CONTINUE
   80 CONTINUE
      RETURN
      END



      SUBROUTINE ELMSTI(WI,HI,IELEM,JELEM,STIFF,ELCOD,THICK
     , ,YOUNG,POISS,DMAT,XINEL,ATMEL,NELEM,MELEM)
      IMPLICIT REAL*8(A-H,O-Z)
      REAL MAPSP(8)
      DIMENSION GAUSBX(2)   ,GAUSBY(2)   ,GUMM(5,8)
      DIMENSION XJACI(2,2)  ,ELCOD(2,8)
      DIMENSION DEMAP(2,8)  ,POSGP(3),WEIGP(3)
      DIMENSION CFB(8,12), SPL(12,24) ,GUMCF(5,12),BMTRIX(5,24)
      DIMENSION BTTRIX(24,5) ,DMAT(5,5),CFBF(1,2),SPLF(2,8)
```

```
      DIMENSION BTD(24,5),BTDB(24,24),STIFF(24,24)
      DO 82 IESTIF=1,24
      DO 82 JESTIF=1,24
   82  STIFF(IESTIF,JESTIF)=0.0D0
      DO 199 I=1,2
      GAUSBX(I) = 0.0D0
   199  GAUSBY(I) = 0.0D0
        NGAUX=1
        CALL GAUSSQ(NGAUX,POSGP,WEIGP)
      DO 201  IGUSS = 1,NGAUX
        POSGPI=POSGP(IGUSS)
        WEIGPI=WEIGP(IGUSS)
      GAUSBX(IGUSS) = XINEL+(1.0D0+POSGPI)/NELEM
         GASX=GAUSBX(IGUSS)
        NGAUY=2
        CALL GAUSSQ(NGAUY,POSGP,WEIGP)
      DO 202 JGUSS  = 1,NGAUY
        POSGPJ=POSGP(JGUSS)
        WEIGPJ=WEIGP(JGUSS)
      GAUSBY(JGUSS) = ATMEL+(1.0D0+POSGPJ)/MELEM
         GASY=GAUSBY(JGUSS)
      CALL SFR2(GASX,GASY,DEMAP,MAPSP)
      CALL JACOB2(ELCOD,DEMAP,XJACI,IELEM,JELEM,DJACB)
      CALL MPTRNB(XJACI,GUMM)
      CALL CBLFB(WI,XINEL,GASX,CFB,CFBF)
      CALL SPLINE(HI,ATMEL,GASY,JELEM,MELEM,SPL,SPLF)
      CALL MATMUL(GUMM,5,8,CFB,12,GUMCF)
      CALL MATMUL(GUMCF,5,12,SPL,24,BMTRIX)

C
C     TRANSFER OF "B" MATRIX
C
      CALL TRMTIX(5,24,BMTRIX,BTTRIX)

C--------MAKE 'D' MATRIX

      CALL DMTRIX(YOUNG,POISS,THICK,DMAT)
      CALL MATMUL(BTTRIX,24,5,DMAT,5,BTD)
      CALL MATMUL(BTD,24,5,BMTRIX,24,BTDB)
      DO 83 IN=1,24
```

```
      DO 83 JN=1,24
   83  STIFF(IN,JN)=STIFF(IN,JN)+BTDB(IN,JN)*DJACB*0.1250D0**2
     , *WEIGPI*WEIGPJ
  202  CONTINUE
  201  CONTINUE
      RETURN
      END


      SUBROUTINE SFR2 (XI, ETA,DEMAP,MAPSP)
      IMPLICIT REAL*8(A-H,O-Z)
      REAL MAPSP(8)
C
C     EVALUATES MAPPING FUNCTIONS AND FOR SIMPLIFIED CUBIC
C     SERENDIPITY ELEMENT
C
      DIMENSION DEMAP(2,8)
      DO 333 I=1,2
      DO 333 J=1,8
  333  DEMAP(I,J) = 0.0D0

C
C     MAPPING FUNCTION MAPSP(XI,ETA) FOR 8 NODED ELEMENT
C

      ETA2 = ETA**2
      MAPSP(1)=1.0D0/32.0D0*(1.0D0-XI)*(9.0D0*ETA2-1.0D0)*(1.0D0+ETA)
      MAPSP(2)=9.0D0/32.0D0*(1.0D0-XI)*(1.0D0-ETA2)*(1.0D0+3.0D0*ETA)
      MAPSP(3)=9.0D0/32.0D0*(1.0D0-XI)*(1.0D0-ETA2)*(1.0D0-3.0D0*ETA)
      MAPSP(4)=1.0D0/32.0D0*(1.0D0-XI)*(9.0D0*ETA2-1.0D0)*(1.0D0-ETA)
      MAPSP(5)=1.0D0/32.0D0*(1.0D0+XI)*(9.0D0*ETA2-1.0D0)*(1.0D0-ETA)
      MAPSP(6)=9.0D0/32.0D0*(1.0D0+XI)*(1.0D0-ETA2)*(1.0D0-3.0D0*ETA)
      MAPSP(7)=9.0D0/32.0D0*(1.0D0+XI)*(1.0D0-ETA2)*(1.0D0+3.0D0*ETA)
      MAPSP(8)=1.0D0/32.0D0*(1.0D0+XI)*(9.0D0*ETA2-1.0D0)*(1.0D0+ETA)

C
C     MAPSP FUNCTION DERIVATIVES
C

     DEMAP(1,1) = -1.0D0/32.0D0*(9.0D0*ETA2-1.0D0)*(1.0D0+ETA)
```

```
      DEMAP(1,2) = -9.0D0/32.0D0*(1.0D0-ETA2)*(1.0D0+3.0D0*ETA)
      DEMAP(1,3) = -9.0D0/32.0D0*(1.0D0-ETA2)*(1.0D0-3.0D0*ETA)
      DEMAP(1,4) = -1.0D0/32.0D0*(9.0D0*ETA2 - 1.0D0)*(1.0D0-ETA)
      DEMAP(1,5) =  1.0D0/32.0D0*(9.0D0*ETA2 - 1.0D0)*(1.0D0-ETA)
      DEMAP(1,6) =  9.0D0/32.0D0*(1.0D0-ETA2)*(1.0D0-3.0D0*ETA)
      DEMAP(1,7) =  9.0D0/32.0D0*(1.0D0-ETA2)*(1.0D0+3.0D0*ETA)
      DEMAP(1,8) =  1.0D0/32.0D0*(9.0D0*ETA2 - 1.0D0)*(1.0D0+ETA)
      DEMAP(2,1)=1.0D0/32.0D0*(1.0D0-XI)*(27.0D0*ETA2+18.0D0*ETA-1.0D0)
      DEMAP(2,2)=-9.0D0/32.0D0*(1.0D0-XI)*(9.0D0*ETA2+2.0D0*ETA-3.0D0)
      DEMAP(2,3)=9.0D0/32.0D0*(1.0D0-XI)*(9.0D0*ETA2-2.0D0*ETA-3.0D0)
      DEMAP(2,4)=-1.0D0/32.0D0*(1.0D0-XI)*(27.0D0*ETA2-18.0D0
     1 *ETA-1.0D0)
      DEMAP(2,5)=-1.0D0/32.0D0*(1.0D0+XI)*(27.0D0*ETA2-18.0D0
     1 *ETA-1.0D0)
      DEMAP(2,6)=9.0D0/32.0D0*(1.0D0+XI)*(9.0D0*ETA2-2.0D0*ETA-3.0D0)
      DEMAP(2,7)=-9.0D0/32.0D0*(1.0D0+XI)*(9.0D0*ETA2+2.0D0*ETA-3.0D0)
      DEMAP(2,8)=1.0D0/32.0D0*(1.0D0+XI)*(27.0D0*ETA2+18.0D0*ETA-1.0D0)
      RETURN
      END


      SUBROUTINE GAUSSQ(NGAU,POSGP,WEIGP)
      IMPLICIT REAL*8(A-H,O-Z)
      DIMENSION POSGP(3),WEIGP(3)
      GOTO (1,2,3) NGAU
1     POSGP(1) = 0.0
      WEIGP(1) = 2.0
      RETURN
2     POSGP(1) = -0.577350269189626
      POSGP(2) = +0.577350269189626
      WEIGP(1) = 1.0
      WEIGP(2) = 1.0
      RETURN
3     POSGP(1) = -0.774596669241483
      POSGP(2) = 0.0D0
      POSGP(3) = +0.774596669241483
      WEIGP(1) = 0.555555555555556
      WEIGP(2) = 0.888888888888889
      WEIGP(3) = 0.555555555555556
```

```
      RETURN
      END


      SUBROUTINE JACOB2(ELCOD,DEMAP,XJACI,IELEM,JELEM,DJACB)
      IMPLICIT REAL*8(A-H,O-Z)
C
C     EVALUATE JACOBIAN MATRIX AND ITS  INVERSE
C     SHAPE FUNCTION DERIVATIVES AT PRESENT SAMPLING POINT
C
      DIMENSION XJACM(2,2), XJACI(2,2) , ELCOD(2,8)
      DIMENSION DEMAP(2,8)
      DO 4 IDIME =1,2
      DO 4 JDIME =1,2
      XJACM(IDIME,JDIME) = 0.0D0
    4 XJACI(IDIME,JDIME) = 0.0D0
      DO 44 IDIME = 1,2
      DO 44 JDIME = 1,2
      DO 44 INODE =1,8
      XJACM(IDIME,JDIME)=XJACM(IDIME,JDIME) +DEMAP(IDIME,INODE)*
     , ELCOD(JDIME,INODE)
   44 CONTINUE

C
C     CALCULATE DETERMINATE AND INVERSE OF JACOBIAN MATRIX
C

      DJACB=XJACM(1,1) * XJACM(2,2) - XJACM(1,2) * XJACM(2,1)
      IF (DJACB) 6,6,8
    6 WRITE(6,900) IELEM ,JELEM
      STOP
    8 CONTINUE
      XJACI(1,1) = XJACM(2,2)/DJACB
      XJACI(2,2) = XJACM(1,1)/DJACB
      XJACI(1,2) = -XJACM(1,2)/DJACB
      XJACI(2,1) = -XJACM(2,1)/DJACB
  900 FORMAT('PROGRAM HEATED IN SUBROUTINE JACOB2',2I4)
      RETURN
      END
```

```
      SUBROUTINE MPTRNB(XJACI,GUMM)
      IMPLICIT REAL*8(A-H,O-Z)
      DIMENSION XJACI(2,2),GUMM(5,8)
      DO 10 I=1,5
      DO 10 J=1,8
10    GUMM(I,J) = 0.0D0
      GUMM(1,1) = XJACI(1,1)
      GUMM(1,2) = XJACI(1,2)
      GUMM(2,3) = XJACI(2,1)
      GUMM(2,4) = XJACI(2,2)
      GUMM(3,1) = XJACI(2,1)
      GUMM(3,2) = XJACI(2,2)
      GUMM(3,3) = XJACI(1,1)
      GUMM(3,4) = XJACI(1,2)
      GUMM(4,5) = 1.0D0
      GUMM(4,7) = XJACI(1,1)
      GUMM(4,8) = XJACI(1,2)
      GUMM(5,6) = 1.0D0
      GUMM(5,7) = XJACI(2,1)
      GUMM(5,8) = XJACI(2,2)
      RETURN
      END

      SUBROUTINE CBLFB(B,XINELI,XI,CFB,CFB2)
      IMPLICIT REAL*8(A-H,O-Z)
      DIMENSION CFB(8,12),CFB2(1,2)
      DO 100 II= 1,8
      DO 100 JJ= 1,12
100   CFB(II,JJ) = 0.0D0
      DO 110 II= 1,1
      DO 110 JJ= 1,2
110   CFB2(II,JJ)= 0.0D0
      AXIL  = (XI - XINELI)/B
      CFB(1,1) = -1.0D0/ B
      CFB(2,2) = 1.0D0 - AXIL
      CFB(3,3) = -1.0D0/ B
      CFB(4,4) = 1.0D0 - AXIL
      CFB(5,1) = 1.0D0 - AXIL
      CFB(6,3) = 1.0D0 - AXIL
```

```
      CFB(7,5) = -1.0D0 / B
      CFB(8,6) = 1.0D0 - AXIL
      CFB(1,7) = 1.0D0 / B
      CFB(2,8) = AXIL
      CFB(3,9) = 1.0D0/B
      CFB(4,10)= AXIL
      CFB(5,7) = AXIL
      CFB(6,9) = AXIL
      CFB(7,11)= 1.0D0/B
      CFB(8,12)= AXIL
C--------CFB2 FOR THE USE OF FORCE MATRIX FOR UNIFORM LOAD
      CFB2(1,1) = 1.0-AXIL
      CFB2(1,2) = AXIL
      RETURN
      END


      SUBROUTINE SPLINE(H,ATMELI,GAU,JELEM,MELEM,SPL,SPL2)
      IMPLICIT REAL*8(A-H,O-Z)
      DIMENSION SPL(12,24),ETK(2),SPL2(2,8)
      H2=H**2
      H3=H**3
      DO 50 II=1,2
      ETK(II) = ATMELI + (II-1)*H
   50 CONTINUE
      DO 100 IN= 1,12
      DO 100 JN= 1,24
  100 SPL(IN,JN) = 0.0D0
      DO 101 IN= 1,2
      DO 101 JN= 1,8
  101 SPL2(IN,JN)= 0.0D0
      DO 110 I=1,7,6
      J = 2*I-1
      SPL(I,J)   = (ETK(2) -GAU )**3/6.0D0/H3
      SPL(I,J+1) = (H3+3*H2*(ETK(2)-GAU)+3.0D0*H*(ETK(2)-GAU)**2-
     ' 3.0D0*(ETK(2)-GAU)**3)/6.0D0/H3
      SPL(I,J+2) = (H3+3*H2*(GAU-ETK(1))+3*H*(GAU-ETK(1))**2-
     ' 3.0D0*(GAU-ETK(1))**3)/6.0D0/H3
      SPL(I,J+3) = (GAU-ETK(1))**3/6.0/H3
      SPL(I+1,J) =-(ETK(2)-GAU)**2/2.0/H3
```

```
      SPL(I+1,J+1)= (9.0*(ETK(2)-GAU)**2 -6.0*H*(ETK(2)-GAU)-3.0*H2
     ' )/6.0/H3
      SPL(I+1,J+2)=(3.0*H2 +6.0*H*(GAU-ETK(1)) - 9.0*(GAU-ETK(1))
     ' **2)/6.0/H3
      SPL(I+1,J+3)=(GAU-ETK(1))**2/2.0/H3
      SPL(I+2,J+4)= SPL(I,J)
      SPL(I+2,J+5)= SPL(I,J+1)
      SPL(I+2,J+6)= SPL(I,J+2)
      SPL(I+2,J+7)= SPL(I,J+3)
      SPL(I+3,J+4)= SPL(I+1,J)
      SPL(I+3,J+5)= SPL(I+1,J+1)
      SPL(I+3,J+6)= SPL(I+1,J+2)
      SPL(I+3,J+7)= SPL(I+1,J+3)
      SPL(I+4,J+8)= SPL(I,J)
      SPL(I+4,J+9)= SPL(I,J+1)
      SPL(I+4,J+10)= SPL(I,J+2)
      SPL(I+4,J+11)= SPL(I,J+3)
      SPL(I+5,J+8)= SPL(I+1,J)
      SPL(I+5,J+9)= SPL(I+1,J+1)
      SPL(I+5,J+10)= SPL(I+1,J+2)
      SPL(I+5,J+11)= SPL(I+1,J+3)
C--------SPL2 FOR THE FORCE MATRIX FOR THE NUIFORM LOAD
      SPL2(1,1)  = (ETK(2) -GAU )**3/6.0/H3
      SPL2(1,2)  = (H3+3*H2*(ETK(2)-GAU)+3*H*(ETK(2)-GAU)**2-
     ' 3.0*(ETK(2)-GAU)**3)/6.0/H3
      SPL2(1,3)  = (H3+3*H2*(GAU-ETK(1))+3*H*(GAU-ETK(1))**2-
     ' 3.0*(GAU-ETK(1))**3)/6.0/H3
      SPL2(1,4)  = (GAU-ETK(1))**3/6.0/H3
      SPL2(2,5)  = SPL2(1,1)
      SPL2(2,6)  = SPL2(1,2)
      SPL2(2,7)  = SPL2(1,3)
      SPL2(2,8)  = SPL2(1,4)
  110 CONTINUE
      RETURN
      END

      SUBROUTINE DMTRIX(YOUNG,POISS,THICK,DMAT)
      IMPLICIT REAL*8(A-H,O-Z)
      DIMENSION DMAT(5,5)
C
```

```
C     EVALUATE D MATRIX  FOR BENDING
C
      DO 5 ISTRE=1,5
      DO 5 JSTRE=1,5
      DMAT(ISTRE,JSTRE)=0.0D0
   5  CONTINUE
      E = YOUNG
      V = POISS
      T = THICK
      T3= T**3
      V2= V**2
      DMAT(1,1)= E*T3/12.0D0/(1.0D0-V2)
      DMAT(1,2)= V*DMAT(1,1)
      DMAT(2,2)= DMAT(1,1)
      DMAT(2,1)= DMAT(1,2)
      DMAT(3,3)= (1.0D0-V)*DMAT(1,1)/2.0D0
      DMAT(4,4)= E*T/(2.433D0*(1.0D0+V))
      DMAT(5,5)= DMAT(4,4)
      RETURN
      END


      SUBROUTINE DEFORM(DISMA,THETAX,THETAY,W)
      IMPLICIT REAL*8(A-H,O-Z)
      DIMENSION DISMA(297,1)
      DIMENSION THETAX(81), THETAY(81), W(81)
      DO 700 I=1,89,11
      DO 690 J=I+1, I+9
      THETAX(J)=1.0D0/6.0D0*(DISMA(J-1,1)+DISMA(J+1,1)
     , +4.0D0*DISMA(J,1))
  690 CONTINUE
  700 CONTINUE
      DO 680 I=100,188,11
      DO 670 J=I+1, I+9
      JJ=J-99
      THETAY(JJ)=1.0D0/6.0D0 *(DISMA(J-1,1)+DISMA(J+1,1)
     , + 4.0D0 * DISMA(J,1))
  670 CONTINUE
  680 CONTINUE
      DO 660 I=189,287,11
```

```
      DO 650 J=I+1, 1+9
      JJ=J-198
      W(JJ)=1.0D0/6.0D0*(DISMA(J-1,1)+DISMA(J+1,1)+4.0D0*DISMA(J,1))
  650 CONTINUE
  660 CONTINUE
      WRITE(6,666)
  666 FORMAT(/,2X,'NODE',14X,'DW/DX',16X,'DW/DY',16X,'W',/)
      DO 701 I=1,89,11
      DO 691 J=I+1, I+9
      WRITE(6,541) J,THETAX(J),THETAY(J),W(J)
  541 FORMAT(2X,I3,10X,F15.5,10X,F15.5,10X,F15.5)
  691 CONTINUE
  701 CONTINUE
      RETURN
      END



      SUBROUTINE BENDMO(DISMA,ELCOD,NELEM,MELEM,WI,HI,DMAT)
      IMPLICIT REAL*8(A-H,O-Z)
      REAL MAPSP(8)
      DIMENSION DISMA(297,1),DMAT(5,5),X(2),Y(2)
      DIMENSION CFB(8,12), SPL(12,24) ,GUMCF(5,12),BMTRIX(5,24)
      DIMENSION DB(5,24),DIS(24,1),DBS(5,1)
      DIMENSION XINEL(8), ATMEL(8),CFB2(1,2),SPL2(2,8)
      DIMENSION GUMM(5,8),XJACI(2,2),ELCOD(2,8)
      DIMENSION DEMAP(2,8)
      WRITE(6,321)
  321 FORMAT(/,'================================================',/
     , ,10X,'STRESS IN THE STRIP',/)
      DO 111 I=1,8
      XINEL(I) = 0.0D0
  111  ATMEL(I) = 0.0D0
      DO 100 IELEM = 1,NELEM
      DO 110 JELEM = 1,MELEM
      DO 112 I = 1,24
  112  DIS(I,1) = 0.0D0
      DO 113 I = 1,5
  113  DBS(I,1) = 0.0D0
      CALL LOGIC3(DISMA,DIS,NELEM,MELEM,IELEM,JELEM)
```

```
      DO 200 I=1,2
      DO 200 J=1,2
      X(I) = 0.0D0
      Y(J) = 0.0D0
200   CONTINUE
      NEI = 2* IELEM -1
      MEI = 2* JELEM -1
      XINEL(IELEM) = -1.0D0 + WI/2 * NEI
      ATMEL(JELEM) = -1.0D0 + HI/2 * MEI
      DO 130 IP=1,2
      X(IP) = XINEL(IELEM) + ((-1)**IP) * 0.577350269*WI /2.0
      DO 131 JP=1,2
      Y(JP) = ATMEL(JELEM) + ((-1)**JP) * 0.577350269*HI /2.0
      WRITE(6,331) X(IP),Y(JP)
331   FORMAT('X(IP)=',F12.4,'Y(JP)=',F12.4,3X,2F12.5)
      CALL SFR2(X(IP),Y(JP),DEMAP,MAPSP)
      CALL JACOB2(ELCOD,DEMAP,XJACI,IELEM,JELEM,DJACB)
      CALL MPTRNB(XJACI,GUMM)
           XINELI= XINEL (IELEM)
       CALL CBLFB(WI,XINELI,X(IP),CFB,CFB2)
           ATMELI= ATMEL (JELEM)
       CALL SPLINE(HI,ATMELI,Y(JP),JELEM,MELEM,SPL,SPL2)
      CALL MATMUL(GUMM,5,8,CFB,12,GUMCF)
      CALL MATMUL(GUMCF,5,12,SPL,24,BMTRIX)
      CALL MATMUL(DMAT,5,5,BMTRIX,24,DB)
      CALL MATMUL(DB,5,24,DIS,1,DBS)
      WRITE(6,332) IELEM,JELEM,(DBS(I,1),I=1,3)
332   FORMAT(I2,3X,I2,3X,3F15.7,/)
131   CONTINUE
130   CONTINUE
110   CONTINUE
100   CONTINUE
      RETURN
      END


      SUBROUTINE TRMTIX(I,J,A,B)
      IMPLICIT REAL*8(A-H,O-Z)
      DIMENSION  A(I,J),B(J,I)
      DO 10 II=1,I
```

```
      DO 10 JJ=1,J
      B(JJ,II)=A(II,JJ)
10    CONTINUE
      RETURN
      END


      SUBROUTINE FORCE(N,NF,MF,SF,FORMA)
      IMPLICIT REAL*8(A-H,O-Z)
      DIMENSION FORMA(N,1)
      DO 10 I=1,N
10    FORMA(I,1) = 0.0D0
      II = 99 * (NF-1) + MF
      FORMA(II-1,1) = 1.0D0/6.0D0 * SF
      FORMA(II,1)   = 2.0D0/3.0D0 * SF
      FORMA(II+1,1) = 1.0D0/6.0D0 * SF
      RETURN
      END



      SUBROUTINE FUNIF(N,WI,HI,FORMA,NELEM,MELEM,ELCOD)
      IMPLICIT REAL*8(A-H,O-Z)
      REAL LOAD(3,1)
      REAL MAPSP(8)
      DIMENSION POSGP(3),WEIGP(3),DEMAP(2,8)
      DIMENSION FORMA(297,1),ELCOD(2,8),CFSP(1,8),CFSP2(3,24)
      DIMENSION GFORC(24,1),XI(8),AT(8),CFSP3(24,3)
      DIMENSION GFO(24,1),GAUSBX(2),GAUSBY(2)
      DIMENSION GUMM(5,8),CFB2(1,2),SPL2(2,8)
      DIMENSION XJACI(2,2)
      DIMENSION CFB(8,12), SPL(12,24)
      DO 900 I=1,297
900   FORMA(I,1)=0.0D0
      DO 890 I=1,8
      XI(I) = 0.0D0
890   AT(I) = 0.0D0
      DO 880 IELEM=1,NELEM
      DO 870 JELEM=1,MELEM
      DO 220 IN=1,24
```

```
      GFORC(IN,1) = 0.0D0
  220 CONTINUE
      DO 199 I=1,2
      DO 199 J=1,8
      CFB2(1,I) = 0.0D0
      SPL2(I,J) = 0.0D0
      POSGP(I) = 0.0D0
      WEIGP(I) = 0.0D0
      GAUSBX(I) = 0.0D0
  199 GAUSBY(I) = 0.0D0
      XI(IELEM)=-1.0D0+(IELEM-1)*WI
      AT(JELEM)=-1.0D0+(JELEM-1)*HI
       NGAUX=2
       CALL GAUSSQ(NGAUX,POSGP,WEIGP)
      DO 201  IGUSS = 1,NGAUX
       POSGPI=POSGP(IGUSS)
       WEIGPI=WEIGP(IGUSS)
      GAUSBX(IGUSS) = XI(IELEM)+(1.0D0+POSGPI)/NELEM
        GASX=GAUSBX(IGUSS)
       NGAUY=2
       CALL GAUSSQ(NGAUY,POSGP,WEIGP)
      DO 202 JGUSS  = 1,NGAUY
        DO 556 I=1,8
  556   CFSP(1,I)=0.0D0
       POSGPJ=POSGP(JGUSS)
       WEIGPJ=WEIGP(JGUSS)
      GAUSBY(JGUSS) = AT(JELEM)+(1.0D0+POSGPJ)/MELEM
        GASY=GAUSBY(JGUSS)
      CALL SFR2(GASX,GASY,DEMAP,MAPSP)
      CALL JACOB2(ELCOD,DEMAP,XJACI,IELEM,JELEM,DJACB)
      CALL CBLFB(WI,XI(IELEM),GASX,CFB,CFB2)
      CALL SPLINE(HI,AT(JELEM),GASY,JELEM,MELEM,SPL,SPL2)
      CALL MATMUL(CFB2,1,2,SPL2,8,CFSP)
      DO 119 I=1,3
      DO 119 J=1,24
      CFSP2(I,J) = 0.0D0
      CFSP3(J,I) = 0.0D0
  119 CONTINUE
      DO 120 IM=1,8
      CFSP2(1,IM)  = CFSP(1,IM)
```

```
      CFSP2(2,8+IM) = CFSP(1,IM)
      CFSP2(3,16+IM)= CFSP(1,IM)
  120 CONTINUE
      CALL TRMTIX(3,24,CFSP2,CFSP3)
      CALL YLOAD(LOAD,3)
      DO 100 I=1,24
      DO 110 J=1,1
      GFO(I,J) = 0.0D0
      DO 129 K=1,3
      GFO(I,J)=GFO(I,J)+CFSP3(I,K)*LOAD(K,J)
  129 CONTINUE
  110 CONTINUE
  100 CONTINUE
C     IF (IELEM.EQ.1 .AND. JELEM.EQ.1) THEN
C      WRITE(8,89) ((  GFO(NI,J),J=1,1),NI=1,24)
C  89  FORMAT(1F15.8)
C     ENDIF
      DO 188 IP=1,24
  188 GFORC(IP,1)=GFORC(IP,1)+GFO(IP,1)*DJACB*0.125**2
     , *WEIGPI*WEIGPJ
  202 CONTINUE
  201 CONTINUE
C--------ADD THE ELEMENT FORCE MATRIX TO GLOBE FORCE MATRIX
      CALL LOGIC2(MELEM,IELEM,JELEM,GFORC,FORMA)
  870 CONTINUE
  880 CONTINUE
      RETURN
      END


      SUBROUTINE YLOAD(LOAD,N)
      IMPLICIT REAL*8(A-H,O-Z)
      REAL LOAD(N,1)
      LOAD(1,1) = 0.0D0
      LOAD(2,1) = 0.0D0
      LOAD(3,1) = 1.0D0
      RETURN
      END
```

```
      SUBROUTINE LOGIC(MELEM,IELEM,JELEM,STIFF,SSTIF)
      IMPLICIT REAL*8(A-H,O-Z)
      DIMENSION STIFF(24,24)  ,SSTIF(297,297)
      DO 120 II = 1,9,4
      IB = (99* II -95)/4
      DO 110 JJ = 1,9,4
      JB = (99 * JJ - 95)/4
      DO 100 I=II,II+3
      DO 100 J=JJ,JJ+3
      INN =  JELEM - 1 + (IELEM -1) * (MELEM + 3) + IB + I - II
      JNN =  JELEM - 1 + (IELEM -1) * (MELEM + 3) + JB + J - JJ
100   SSTIF(INN,JNN) = SSTIF(INN,JNN) + STIFF(I,J)
110   CONTINUE
120   CONTINUE
      DO 220 II = 13,21,4
      IB = (99*II -1239) / 4
      DO 210 JJ = 13,21,4
      JB = (99*JJ-1239) /4
      DO 200 I=II,II+3
      DO 200 J=JJ,JJ+3
      INN =  JELEM - 1 + (IELEM -1) * (MELEM + 3) + IB + I - II
      JNN =  JELEM - 1 + (IELEM -1) * (MELEM + 3) + JB + J - JJ
200   SSTIF(INN,JNN) = SSTIF(INN,JNN) + STIFF(I,J)
210   CONTINUE
220   CONTINUE
      DO 320 II = 1,9,4
      IB = (99 * II -95)/4
      DO 310 JJ = 13,21,4
      JB = (99*JJ -1239) /4
      DO 300 I=II,II+3
      DO 300 J=JJ,JJ+3
      INN =  JELEM - 1 + (IELEM -1) * (MELEM + 3) + IB + I - II
      JNN =  JELEM - 1 + (IELEM -1) * (MELEM + 3) + JB + J - JJ
300   SSTIF(INN,JNN) = SSTIF(INN,JNN) + STIFF(I,J)
310   CONTINUE
320   CONTINUE
      DO 420 II = 13,21,4
      IB = (99 * II-1239)/4
      DO 410 JJ = 1,9,4
```

```
      JB = (99*JJ - 95)/4
      DO 400 I=II,II+3
      DO 400 J=JJ,JJ+3
      INN =  JELEM - 1 + (IELEM -1) * (MELEM + 3) + IB + I - II
      JNN =  JELEM - 1 + (IELEM -1) * (MELEM + 3) + JB + J - JJ
  400 SSTIF(INN,JNN) = SSTIF(INN,JNN) + STIFF(I,J)
  410 CONTINUE
  420 CONTINUE
      RETURN
      END



      SUBROUTINE LOGIC2(MELEM,IELEM,JELEM,GFORC,FORMA)
      IMPLICIT REAL*8(A-H,O-Z)
      DIMENSION GFORC(24,1),FORMA(297,1)
      DO 130 II=1,17,8
      IN =(99 * II - 91 ) / 8
      DO 140 I = II, II+3
      INN =  JELEM - 1 + (IELEM -1) * (MELEM + 3) + IN + I - II
      FORMA(INN,1) = FORMA(INN,1) + GFORC(I,1)
  140 CONTINUE
      DO 150 I = II+4, II+7
      INN =  JELEM - 1 + IELEM  * (MELEM + 3) + IN + I - II-4
      FORMA(INN,1) = FORMA(INN,1) + GFORC(I,1)
  150 CONTINUE
  130 CONTINUE
      RETURN
      END


      SUBROUTINE SBOUND(BOUND,SSTIF,N)
      IMPLICIT REAL*8(A-H,O-Z)
      DIMENSION SSTIF(297,297)
      DIMENSION BOUND(3,3)
      BK=5500.0D0
      BOUND(1,1) = BK*1.0D0
      BOUND(1,2) = BK*4.0D0
      BOUND(1,3) = BK*1.0D0
      BOUND(2,1) = BK*4.0D0
```

```
      BOUND(2,2) = BK*16.0D0
      BOUND(2,3) = BK*4.0D0
      BOUND(3,1) = BK*1.0D0
      BOUND(3,2) = BK*4.0D0
      BOUND(3,3) = BK*1.0D0
C
      DO 102 II =0,88,11
      DO 101 I=1,3
      DO 101 J=1,3
      SSTIF(II+I,II+J)       = SSTIF(II+I,II+J) + BOUND(I,J)
      SSTIF(99+II+I,99+II+J) = SSTIF(99+II+I,99+II+J) + BOUND(I,J)
      SSTIF(198+II+I,198+II+J)=SSTIF(198+II+I,198+II+J)+BOUND(I,J)
  101 CONTINUE
  102 CONTINUE

      DO 202 II =1,8
      DO 201 I=1,3
      DO 201 J=1,3
      SSTIF(II+I,II+J)       = SSTIF(II+I,II+J) + BOUND(I,J)
      SSTIF(99+II+I,99+II+J) = SSTIF(99+II+I,99+II+J) + BOUND(I,J)
      SSTIF(198+II+I,198+II+J)=SSTIF(198+II+I,198+II+J)+BOUND(I,J)
  201 CONTINUE
  202 CONTINUE

      DO 302 II =89,96,1
      DO 301 I=1,3
      DO 301 J=1,3
      SSTIF(II+I,II+J)       = SSTIF(II+I,II+J) + BOUND(I,J)
      SSTIF(99+II+I,99+II+J) = SSTIF(99+II+I,99+II+J) + BOUND(I,J)
      SSTIF(198+II+I,198+II+J)=SSTIF(198+II+I,198+II+J)+BOUND(I,J)
  301 CONTINUE
  302 CONTINUE

      DO 104 II =8,86,11
      DO 103 I=1,3
      DO 103 J=1,3
      SSTIF(II+I,II+J)       = SSTIF(II+I,II+J) + BOUND(I,J)
      SSTIF(99+II+I,99+II+J) = SSTIF(99+II+I,99+II+J) + BOUND(I,J)
      SSTIF(198+II+I,198+II+J)=SSTIF(198+II+I,198+II+J)+BOUND(I,J)
  103 CONTINUE
```

```
  104  CONTINUE
       RETURN
       END


       SUBROUTINE LOGIC3(DISMA,DIS,NELEM,MELEM,IELEM,JELEM)
       IMPLICIT REAL*8(A-H,O-Z)
       DIMENSION DISMA(297,1),DIS(24,1)
       DO 100 I =1,9,4
       II = (99*I -95)/4
       DO 110 J = I, I+3
       JJ = (IELEM-1)*(MELEM+3)+(JELEM-1)+II+J-I
  110  DIS(J,1) = DISMA(JJ,1)
  100  CONTINUE
       DO 102 I = 13,21,4
       II = (99*I -1267)/4
       DO 120 J=I,I+3
       JJ = (IELEM)*(MELEM+3)+(JELEM-1)+II+J-I-4
  120  DIS(J,1) = DISMA(JJ,1)
  102  CONTINUE
       RETURN
       END


       SUBROUTINE MATIN(ST,N)
       IMPLICIT REAL*8(A-H,O-Z)
       DIMENSION ST(N,N)
C
C      MATRIX INVENSION
C
       DO 19 I=1,N
       Z=ST(I,I)
       ST(I,I)=1.
       DO 60 J=1,N
   60  ST(I,J)=ST(I,J)/Z
       DO 19 K=1,N
       IF(K-I) 3,19,3
    3  Z=ST(K,I)
       ST(K,I)=0.0D0
       DO 4 J=1,N
```

```
  4   ST(K,J)=ST(K,J)-Z*ST(I,J)
 19   CONTINUE
      RETURN
      END

C
C     MATRIX MULTIPLICATION
C
      SUBROUTINE MATMUL(A,N,M,B,L,C)
      IMPLICIT REAL*8(A-H,O-Z)
      DIMENSION A(N,M),B(M,L),C(N,L)
      DO 100 I=1,N
      DO 110 J=1,L
      C(I,J)=0.0D0
      DO 120 K=1,M
      C(I,J)=C(I,J)+A(I,K)*B(K,J)
  120 CONTINUE
  110 CONTINUE
  100 CONTINUE
      RETURN
      END
```

Appendix B

Data file for present method:

```
1.7416698,2*0.1974992,1.7416698,6.9378222,2*6.10634573,6.9378222
6.5d0,2.2574263,-2.2574263,-6.5d0,-3.5d0,-1.2155372,1.2155372,3.5d0
0.168d0,8,8
460000.0d0,0.35d0
3,6,1.0
```

Data file for finite element method:

```
0.168,460000.0,0.35,0.0
24,93,2,1
1,0,1.7416698,-6.5d0
2,0,2.3911889,-6.125d0
3,0,3.0407080,-5.75d0
4,0,3.6902270,-5.375d0
5,0,4.3397461,-5.0d0
6,0,4.9892651,-4.625d0
7,0,5.6387842,-4.25d0
8,0,6.2883032,-3.875d0
9,0,6.9378227,-3.5d0
10,0,1.2179988,-5.4940374
11,0,2.5774605,-4.8601100
12,0,3.9369222,-4.2261826
13,0,5.2963838,-3.5922552
14,0,6.6558455,-2.9583278
15,0,0.7839959,-4.4462619
16,0,1.4887654,-4.1897468
17,0,2.1935349,-3.9332317
18,0,2.8983043,-3.6767166
19,0,3.6030738,-3.4202015
20,0,4.3078433,-3.1636864
21,0,5.0126127,-2.9071713
22,0,5.7173822,-2.6506561
23,0,6.4221517,-2.3941410
24,0,0.4429643,-3.3646476
25,0,1.8918530,-2.9764190
26,0,3.3407418,-2.5881904
27,0,4.7896305,-2.1999619
28,0,6.2385193,-1.8117333
29,0,0.1974992,-2.2574263
30,0,0.9361050,-2.1271902
31,0,1.6747108,-1.9969540
32,0,2.4133166,-1.8667179
33,0,3.1519225,-1.7364818
```

34,0,3.8905283,-1.6062456
35,0,4.6291341,-1.4760095
36,0,5.3677400,-1.3457734
37,0,6.1063457,-1.2155372
38,0,0.0494689,-1.1330247
39,0,1.5437609,-0.8725524
40,0,3.0380530,-0.6120801
41,0,4.5323445,-0.3516079
42,0,6.0266371,-0.0911356
43,0,0.0d0,0.0d0
44,0,0.75d0,0.0d0
45,0,1.5d0,0.0d0
46,0,2.25d0,0.0d0
47,0,3.0d0,0.0d0
48,0,3.75d0,0.0d0
49,0,4.5d0,0.0d0
50,0,5.25d0,0.0d0
51,0,6.0d0,0.0d0
52,0,0.0494689,1.1330247
53,0,1.5437609,0.8725524
54,0,3.0380530,0.6120801
55,0,4.5323445,0.3516079
56,0,6.0266371,0.0911356
57,0,0.1974992,2.2574263
58,0,0.9361050,2.1271902
59,0,1.6747108,1.9969540
60,0,2.4133166,1.8667179
61,0,3.1519225,1.7364818
62,0,3.8905283,1.6062456
63,0,4.6291341,1.4760095
64,0,5.3677400,1.3457734
65,0,6.1063457,1.2155372
66,0,0.4429643,3.3646476
67,0,1.8918530,2.9764190
68,0,3.3407418,2.5881904
69,0,4.7896305,2.1999619
70,0,6.2385193,1.8117333

71,0,0.7839959,4.4462619
72,0,1.4887654,4.1897468
73,0,2.1935349,3.9332317
74,0,2.8983043,3.6767166
75,0,3.6030738,3.4202015
76,0,4.3078433,3.1636864
77,0,5.0126127,2.9071713
78,0,5.7173822,2.6506561
79,0,6.4221517,2.3941410
80,0,1.2179988,5.4940374
81,0,2.5774605,4.8601100
82,0,3.9369222,4.2261826
83,0,5.2963838,3.5922552
84,0,6.6558455,2.9583278
85,0,1.7416698,6.5d0
86,0,2.3911889,6.125d0
87,0,3.0407080,5.75d0
88,0,3.6902270,5.375d0
89,0,4.3397461,5.0d0
90,0,4.9892651,4.625d0
91,0,5.6387842,4.25d0
92,0,6.2883032,3.875d0
93,0,6.9378227,3.5d0
1,0,1,3,15,17,2,16,10,11
6,14,0,0,0,0,0,0,0,0
7,0,3,5,17,19,4,18,11,12
12,14,0,0,0,0,0,0,0,0
13,0,5,7,19,21,6,20,12,13
18,14,0,0,0,0,0,0,0,0
19,0,7,9,21,23,8,22,13,14
24,14,0,0,0,0,0,0,0,0
1,0,0,18
0,0,0,22
1,2,3,4,5,6,7,8,9,85,86,87,88,89,90,91,92,93
10,15,24,29,38,43,52,57,66,71,80,14,23,28,37,42,51,56,65,70,79,84
43,1,1.0